EXPERIMENTAL EVIDENCE FOR HYSTERESIS IN THE CELL CYCLES OF *XENOPUS LAEVIS* EGG EXTRACTS

Wei Sha

Thesis submitted to the faculty of

Virginia Polytechnic Institute and State University

in partial fulfillment for the requirements for the degree of

Master of Science

In

Biology

Jill Sible, Committee Chair

John Tyson, Committee Co-Chair

Peter Kennelly, Committee Member

Cynthia Gibas, Committee Member

Edward Wojcik, Committee Member

Aug 14, 2002

Blacksburg, Virginia

Key words: Hysteresis, Bistability, Xenopus, MPF, Cyclin B

Experimental Evidence for Hysteresis in the Cell Cycles of *Xenopus Laevis* Egg Extracts

Wei Sha

(ABSTRACT)

In 1993, Novak and Tyson published a comprehensive mathematical model of the regulation of M-phase promoting factor (MPF) activity in *Xenopus laevis* eggs and egg extracts. Although this model was in agreement with existing and subsequent experimental data, fundamental predictions that the cell cycle is driven by a hysteresis loop have never been validated experimentally. The model's predictions of bifurcations that create and destroy MPF activity, indicative of hysteresis, were tested in this study.

Prediction 1: The threshold concentration of cyclin B required to activate MPF is measurably higher than the threshold concentration required to inactivate MPF. The difference in thresholds implies that the MPF control system is hysteretic and bistable. To measure these thresholds, extracts in interphase or M-phase were supplemented with varying concentrations of non-degradable human cyclin B1 protein (Δ87 cyclin B1). MPF activity was determined by the morphology of sperm nuclei and by assays of histone H1 kinase activity. Consistent with the model, the activation threshold was determined to be 40 nM, which is two-fold higher than the inactivation threshold, 20 nM.

Prediction 2: For cyclin levels marginally above the activation threshold concentration of cyclin B, there is a dramatic "slowing-down" in the rate of MPF activation. Supra-threshold concentrations of Δ87 cyclin B1 were added to cycloheximide-treated CSF-released extracts, and samples taken at various time-points were analyzed for MPF activity. At 40 nM cyclin B1, just above the activation threshold, the lag time for MPF activation was 45 - 60 minutes; at 50 nM cyclin B1, the lag time was between 30 - 45 minutes; and at 60 nM or higher concentrations of cyclin B1, the lag time was 20 - 30 minutes, thus confirming the prediction of the Novak-Tyson model.

Prediction 3: DNA replication checkpoint increases the activation threshold concentration of cyclin B by increasing the hysteresis loop. Cycloheximide-treated, CSF-released extracts containing 1200 sperm nuclei/µl were treated with aphidicolin, then supplemented with varying concentrations of Δ87 cyclin B1. The activation threshold was 100 nM, 2.5 fold higher than in extracts lacking aphidicolin.

Conclusions: These studies confirm three predictions of the Novak-Tyson model and indicate that hysteresis underlies cell cycle control in Xenopus egg extracts. These experiments validate use of mathematical models to study complex biological control systems such as the eukayotic cell cycle.

ACKNOWLEDGEMENT

Foremost I would like to express my gratitude to my advisor, Dr. Jill Sible, for her suggestions and instructions on my research, for her support, patience, encouragement, understanding and open mind throughout my graduate studies. Thanks to her for reading previous drafts and making corrections on my thesis. And thanks to her for making this lab a wonderful working environment.

I am grateful to my co-advisor, Dr. John Tyson, for his patient instructions. His broad and profound knowledge has given me a great help on mathematical model and cell cycle.

My thanks also go to my committee members, Dr. Peter Kennelly, Dr. Cynthia Gibas and Dr. Edward Wojcik for sharing their knowledge and providing many valuable comments to this research.

I would like to thank Dr. Chung-Seon Yi for analyzing and fitting my data into the mathematical model.

Furthermore, I would like to thank all the lab members for contributing to such an inspiring and pleasant atmosphere. I will never forget the good times that I spent with my lab friends: Matthew Petrus, Ayesha Carter, Brian Wroble, Ian Auckland, Matt Tormenti, Bob Johnson, Dayna Wilhelm and Tony Lassaletta. Special thanks to Matt Petrus. He never tired of helping others and was always ready to entertain us with a joke or a song. Special thanks to Tony. He has been working with me for one year as an undergraduate student. He was an excellent helper for this project, especially for cell culture and protein purification. Special thanks to Bob for sharing his technical wisdom with Tony and me. He gave us a lot of advice and help on protein expression. I appreciate all former and present Sible lab members for every moment that we have worked together.

I am also grateful to Dr. Kathy Chen for her discussions and notes, but mostly for being such a nice friend. Thanks to her for leaving such a challenging project to me, her previous work made this research easier. We had many inspiring discussions. She taught me many lessons on the workings of academic research in general.

My parents receive my deepest gratitude and love for their dedication.

Financial support has been provided by DOD DARPA-BioSPICE E-1-1874; Division of Research at VT; Carilion Biomedical OSER.

To all of you, thank you.

TABLE OF CONTENTS PAGE

LIST OF FIGURES PAGE

LIST OF TABLES PAGE

Chapter 1: INTRODUCTION

1.1 The Novak-Tyson mathematical model

The cell cycle is an ordered set of processes of cell growth and cell division (proliferation). The cell cycle is divided into four fundamental parts: G1, S, G2 and M phase. During S phase, DNA is replicated. During M phase, the cell divides. In somatic cells, S phase is preceded by a temporal gap called G1 phase and is followed by a gap called G2 phase. G1 and G2 phases are characterized by protein synthesis and cell growth. Unlike somatic cells, G1 and G2 phases are absent in early embryos. The eggs rely on nutrients, RNA and proteins provided maternally and simply subdivide into smaller and smaller cells without any cell growth between cell divisions. The absence of gap phases and growth makes the early embryo a simplified system for the study of cell cycle controls (Murray, 1993).

The cell cycle is precisely controlled. In recent years, more and more cell cycle control proteins have been identified and more and more interactions among these proteins have been unraveled, which makes it increasingly difficult to make reliable predictions by intuitive methods alone. To understand the complex network of cell cycle control, precise mathematical and computational tools are needed to integrate our information.

Based on classical biochemical kinetics and modern dynamical systems theory, Novak and Tyson developed computational models of cell cycle control. By combining the results of many experimental studies of *Xenopus* egg extracts, Novak and Tyson constructed a model of MPF regulation, and then translated the model into precise mathematical equations and studied their properties by accurate numerical simulation. This model predicted that MPF regulation in *Xenopus* eggs or egg extracts is bistable and hysteretic (Novak and Tyson, 1993; Novak and Tyson, 1995; Tyson, 1991).

A nonlinear dynamical system controlled by positive feedback may exist in either of two steady states under identical conditions (bistability), depending upon the path by which it arrived at a particular state (hysteresis). It is predicted that bistability and hysteresis make cell cycle transitions irreversible (for details, see Chapter 2) (Novak and

Tyson, 1993). Although the Novak-Tyson model was in agreement with existing and subsequent experimental data, fundamental predictions that the cell cycle is driven by a hysteresis loop have never been validated experimentally. The prediction of bistability and hysteresis in the MPF control system was tested in this study.

1.2 Physiology of embryonic cell cycles (Fig. 1)

1.2.1 Oocytes

A frog egg develops in several stages. The egg is derived from a much smaller cell known as an oocyte. Soon after its birth in the ovary, the oocyte completes S phase of meiosis and then arrests in G2 for several months, during which it grows gradually to a diameter of about 1 millimeter. This stage is called the immature oocyte. In response to hormonal cues from the pituitary gland, the follicle cells surrounding the oocyte then secrete the hormone progesterone, which interacts with the oocyte to initiate the process of oocyte maturation, during which immature oocytes complete the first meiotic division (Meiosis I) and arrest at metaphase of Meiosis II. This stage is called the mature oocyte (reviewed in Murray and Hunt, 1993).

1.2.2 Fertilized eggs

When maturation is complete, the egg can be fertilized *in vitro* to produce an embryo that divides synchronously through twelve cell cycles. When an egg is fertilized, calcium ions are released through an IP3-gated channel in the endoplasmic reticulum (reviewed by Ciapa et al., 2000). Increased intracellular calcium triggers embryonic cell cycles by first releasing the egg from metaphase of Meiosis II through activation of CaM kinase II (Lorca et al., 1993). The first cell cycle lasts 75 to 90 minutes and is followed by 11 synchronous cell cycles, each of which lasts 20 to 30 minutes. In early embryonic cell cycles, G1 and G2 are absent, and the cell cycle consists of rapid alternations between DNA replication and mitosis. After the twelfth mitosis, the cell cycle slows, and the synchrony among cells breaks down (Satoh 1977). The first 12 rapid divisions quickly subdivide the egg into a hollow ball of 4096 cells, called the blastula, which then

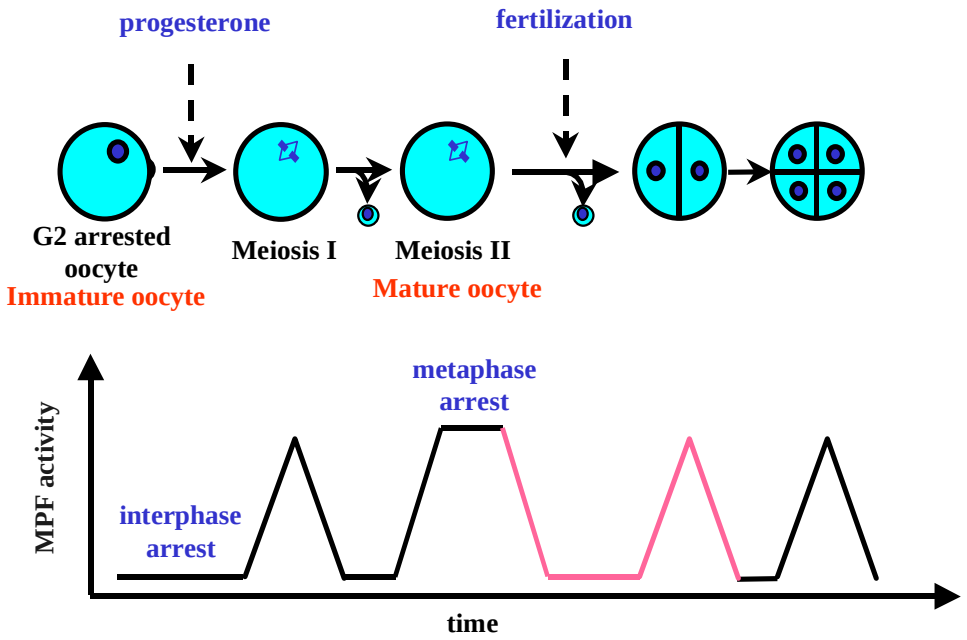

Fig.1. Meiotic and mitotic cell cycles of frog eggs (adapted from Murray & Hunt, 1993, Fig. 2-6). The immature oocyte (far left) is arrested in G2 phase with low MPF activity and replicated chromosomes. Progesterone-induced activation of MPF triggers Meiosis I, during which homologous chromosomes line up on the spindle. The paired chromosomes are separated to the two poles of the spindle as MPF activity drops at the end of meiosis I. One set of chromosomes remains in the egg and the other set is discarded in a small polar body. As MPF activity rises again, the egg enters Meiosis II, with its replicated chromosomes attached again to the spindle. The mature egg arrests in this state, awaiting fertilization. Fertilization triggers destruction of MPF in the egg, coincident with separation of sister chromatids to the two poles of the spindle. One set of chromatids is discarded in a small polar body, and the other set combines with sperm chromatids to reconstitute the diploid state in the fertilized egg. Shortly thereafter, the DNA in each chromosome is replicated and about 90 min after fertilization the egg is driven into Mitosis I by rising MPF activity. Subsequent cycles of MPF activation and inactivation drive a series of rapid, synchronous mitotic divisions to produce a hollow ball of cells, called the blastula. MPF activity is high whenever the eggs are in M phase (meiosis or mitosis); MPF activity is low whenever the eggs are in interphase (S phase).

undergoes complex changes in morphology and gene expression during gastrulation (Dettlaff, 1964; Satoh 1977).

Somatic cells are small, so they have to grow and duplicate all the components of the cell for cell divisison. Eggs, however, are large and inherit a stock of nutrients from their mother, so they do not need to grow between cell divisions. This explains why eggs can divide without growing and why early embryonic cell cycles are faster than somatic cell cycles (Murray and Hunt, 1993).

1.2.3 Egg extracts

Frog oocytes and eggs are useful model systems for studies of the cell cycle. Because amphibian eggs are large, they provide the advantages of easy microinjection and the ability to perform biochemical analysis on microinjected cells. However, microinjection allows only a limited variety of perturbations of the cell cycle. Microinjection can only be performed before cell division; the amount of the eggs that can be handled and the number of proteins that can be manipulated at the same time are very limited. Moreover, the refractory nature of the yolk platelets makes microscopic examination of intracellular events in living frog embryos difficult (Murray, 1991). These problems have been overcome by the development of egg extracts. Lohka and Masui (1983) first described a method of centrifuging eggs to produce extracts. Murray and Kirschner (1989) developed egg extracts that could undergo multiple cell cycles *in vitro*. Frog egg extracts can be made from thousands of eggs to provide enough volume for complex biochemical experiments. In frog egg extracts, levels of cyclins (proteins that are periodically synthesized and degraded throughout the cell cycle and are the regulatory subunits of cyclin dependent kinases), Cdks (cyclin dependent kinases which regulate cell cycle by phosphorylating other proteins) and regulatory molecules can be manipulated at any time of the cell cycle, and the activation and phosphorylation states of the Cdks can be monitored over time. For these reasons, egg extracts are convenient preparations for testing theoretical predictions of bistability and hysteresis.

Two different types of *Xenopus* egg extracts have been used to test this mathematical model. 1) CSF extract is an extract that contains cytostatic factor (CSF)

which arrests the extract in Meiosis II (Murray and Kirschner, 1989; Murray et al., 1989). A CSF extract activated by calcium is called a CSF-released extract. Calcium activation is used to mimic fertilization. Although, the molecular composition of CSF is still not fully understood, the Mos/MAPK signaling pathway is thought to be a component of CSF. Fertilization induces degradation of c-Mos (a protein kinase) (Watanabe et al., 1991; Lorca et al., 1993; Roy et al., 1996). The biological activity of c-Mos is mediated by activation of a MAP kinase (MAPK) cascade through the phosphorylation of the MAPK-activating kinase, MEK (Nebreda and Hunt, 1993; Posada et al., 1993; Shibuya and Ruderman, 1993). In Meiosis II, the c-Mos/MAPK pathway inhibits APC-dependent proteolysis of cyclin B (Abrieu et al., 1997; Bhatt and Ferrell, 1999; Cross et al., 2000). Thus, c-Mos-dependent activation of MAPK plays an important role in maintaining a stable metaphase arrest necessary for mature eggs awaiting fertilization (Haccard et al., 1993; Colledge et al., 1994). 2) A cycling extract is an extract that is activated by calcium ionophore prior to crushing. This extract starts from the first interphase, and usually can cycle through two or more mitosis.

1.3 Molecular mechanisms of embryonic cell cycles

1.3.1 MPF and its function

MPF, maturation-promoting factor or mitosis-promoting factor, is the key regulator of the cell cycle. MPF promotes the onset of meiotic maturation in immature oocytes and promotes the onset of mitosis in diploid cells. In 1988, Lohka et al. purified and identified MPF as a dimer comprised of Cdc2 and cyclin B (Lohka et al., 1988). In active MPF, Cdc2 is bound to cyclins B1 and B2 (Gautier et al., 1990). Cdc2 is a cyclin-dependent kinase (Cdk) that, when activated, phosphorylates a variety of proteins. Thus, MPF functions by adding phosphates onto specific proteins. One such target is histone H1, which is bound to DNA (Langan et al., 1989). The phosphorylation of this protein may result in chromosomal condensation, a useful indicator of M phase. Another target of MPF is the nuclear envelope. Purified MPF phosphorylates nuclear envelope proteins and brings about their depolymerization *in vitro* (Peter et al., 1990; Ward and Kirschner, 1990). After the addition of MPF, the lamin proteins of the nuclear envelope become

hyperphosphorylated. Nuclear envelope then depolymerizes and breaks apart (Miake-Lye and Kirschner, 1985; Arion et al., 1988). Nuclear envelope breakdown is another important indicator of M phase. A third target is RNA polymerase (Cisek and Corden, 1989; Leresche et al., 1996), whose phosphorylation is responsible for the inhibition of transcription during mitosis. A fourth target of MPF is the regulatory subunit of cytoplasmic myosin (Yamashiro et al., 1991). When phosphorylated, myosin becomes inactive and is unable to function as an ATPase to drive the actin filaments involved in cell division (Satterwhite et al., 1992). The inhibition of this myosin during the early stages of mitosis may prevent cell division before chromosomes separation.

Cyclin A also forms active kinase complexes with Cdc2. These complexes have a G2/M function in mammalian somatic cell cycles (Pagano et al., 1992) and also participate in S/M checkpoint control in Xenopus embryonic cycles (Walker and Maller, 1991).

Like Cdc2, Cdk2 is another cyclin dependent kinase. In higher eukaryotes Cdk2 plays an essential role in control of S phase (Blow and Nurse, 1990; Fang and Newport, 1991) and is regulated by A- and E-type cyclins. A number of observations suggest that cyclin E/cdk2 complexes are required for initiation of S phase. Cyclin E is periodically expressed during the cell cycle and maximally activates Cdk2 at the G1/S transition (Dulic et al., 1992; Koff et al., 1992).

1.3.2 How is MPF activity regulated? (Fig. 2)

Cdc2 has no kinase activity unless it is associated with cyclins. The cyclins enable the Cdc2 kinase subunit to become phosphorylated at residues threonine-14 (T-14), tyrosine-15 (Y-15), and threonine-161 (T-161). The phosphorylation at T-161 by CAK (Cdk-activating kinase) is necessary for MPF activity (Solomon, 1994), while phosphorylations at T-14 and Y-15 inhibit MPF kinase activity (Draetta et al., 1989; Dunphy and Newport, 1989). Thus, when phosphorylated in these three positions, the kinase remains inactive but potentially functional. The potentially functional MPF molecules (pre-MPF) accumulate during the late S period. The phosphorylation state of

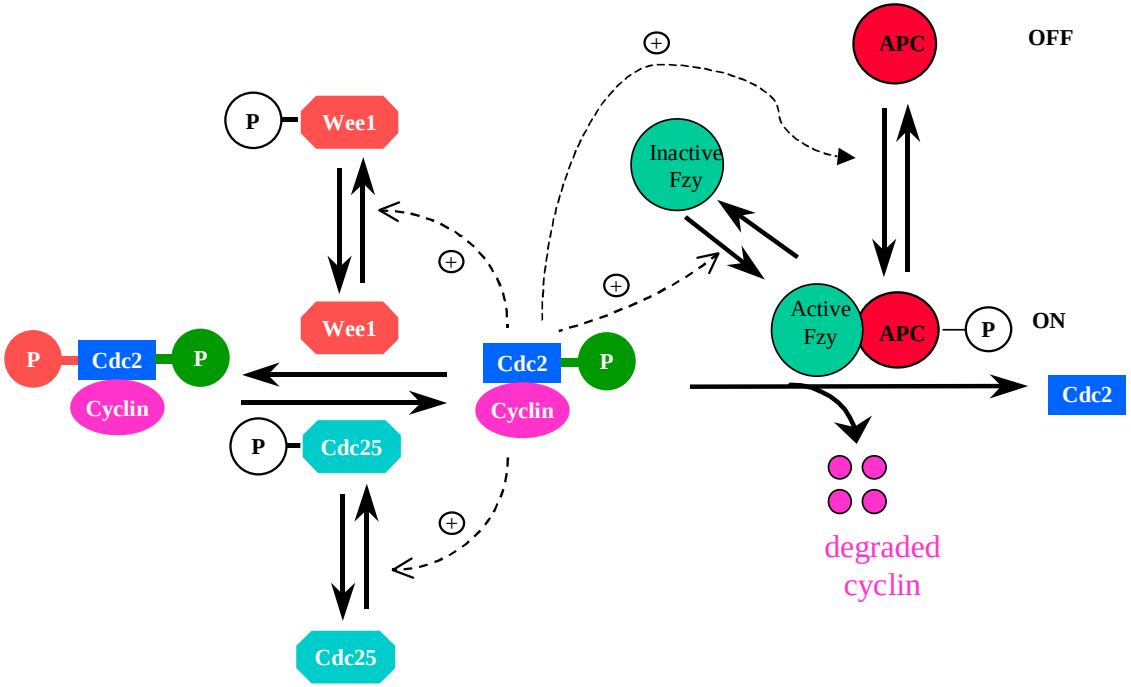

Fig.2. A model of the cell cycle engine in frog eggs. Wee1 is inactivated and Cdc25 is activated by phosphorylation. Active MPF promotes these phosphorylation events directly, forming two positive feedback loops. Cyclin degradation is initiated by the anaphase promoting complex (APC) which has to bind to Fzy to be activated. MPF activates APC directly and activates Fzy indirectly, forming a negative feedback loop. (The feedback loops are adapted from Novak and Tyson, 1993)

Y15 and T14 is controlled by Wee1, Myt1 and Cdc25. The inhibitory phosphorylations are carried out by protein kinases, Wee1 and Myt1, which act on Y15 or both Y15 and T14, respectively (Featherstone and Russell, 1991; Parker and Piwnica-Worms, 1992; McGowan and Russell, 1995; Mueller et al., 1995a, b; Watanabe et al., 1995). The dephosphorylation of these residues, which activates Cdc2, is catalyzed by protein phosphatase Cdc25 (Dunphy and Kumagai, 1991; Gautier et al., 1991). Wee1 phosphorylated on some residues is less active (Mueller et al., 1995), and Cdc25 phosphorylated on some residues is more active than the unphosphorylated forms (Gautier et al., 1991 and Kumagai et al., 1991). Cdc2 can phosphorylate Wee1 and Cdc25 on these residues (Coleman and Dunphy, 1994) to inactivate Wee1 (Smythe and Newport, 1992) and activate Cdc25 (Kumagai and Dunphy, 1992; Izumi and Maller, 1993), forming two positive feedback loops involving MPF activation.

To exit mitosis, the cyclin subunit of MPF must be destroyed by the ubiquitin pathway of proteolysis (Glotzer et al., 1991). First, a ubiquitin-activating enzyme, E1, uses the energy of ATP hydrolysis to form a thiolester bond with ubiquitin. Next, activated ubiquitin is transferred to a ubiquitin-carrier protein, E2. Finally, ubiquitin is transferred to the protein substrate, which is cyclin B in this case, by the action of a ubiquitin-protein ligase, E3 (King et al., 1995; Sudakin et al., 1995). The regulated component of the mitotic cyclin ubiquitination system, activated at the metaphase-to-anaphase transition, is the large E3 complex, known as the cyclosome (Sudakin et al., 1995) or the anaphase-promoting complex (APC) (King et al., 1995). The latter name derives from the finding that components of the APC are essential for anaphase progression in many organisms. Cdc2/cyclin B kinase has been shown to turn on the cyclin degradation pathway in *Xenopus* egg extracts (Felix et al., 1990). Cdc2/cyclin B activates APC at the end of mitosis by direct phosphorylation (Patra and Dunphy, 1998). In addition to phosphorylation, the presence of the Fzy protein is also necessary for full activation of APC in *Xenopus* egg extracts (Lorca et al., 1998). Active MPF activates Fzy by triggering the degradation of Emi1, an intermediate protein which binds to and inhibits Fzy during interphase (Reimann et al., 2001). The activated APC attaches ubiquitin

molecules to cyclin B protein, ubiquitin-labeled cyclin B protein is then recognized by proteasomes and broken down, which results in low MPF activity and exit from mitosis.

Cdk inhibitory proteins (CKIs) are another type of Cdk-cyclin regulators which can bind and inactivate some Cdk-cyclin complexes. In *Xenopus* eggs, two closely related (probably functionally equivalent) CKIs have been identified, called Xic1 (Su et al., 1995) and Kix (Shou and Dunphy, 1996). Xic1 is only degraded when bound to cyclin E/Cdk2, which is associated with replication origin proteins on the DNA (Furstenthal et al, 2001). Xic1 degradation in *Xenopus* egg extracts is coupled to initiation of DNA replication (You et al., 2002). However, neither Xic1 nor Kix is present in early embryos.

Therefore, MPF activity in *Xenopus* egg extracts is regulated by two factors: 1) Cdc2 phosphorylation and dephosphorylation. 2) cyclin B synthesis and degradation.

In the Novak and Tyson model (1993), two major feedback signals govern the MPF regulatory system: 1) MPF modulates the kinase (Wee1) and phosphatase (Cdc25) that regulate its own activity, in positive feedback loops; 2) MPF stimulates the proteolytic machinery that degrades cyclin subunits and destroys MPF activity, thereby creating a negative feedback loop.

The positive feedback loops create hysteresis loops and account for thresholds and time lags in cyclin-induced activation of MPF. The negative feedback loop is consistent with observed time lags in MPF-induced cyclin degradation (Novak and Tyson, 1993). Positive and negative feedback loops work together to create MPF oscillations.

1.3.3 Cyclin B level and MPF activity

1.3.3.1 Activation threshold concentration of cyclin B and lag time

In 1989, Murray and coworkers showed that cyclin B synthesis and degradation correlate closely with MPF activation and inactivation. They demonstrated that synthesis and degradation of cyclin B is necessary and sufficient to drive cell cycles in egg extracts (Murray et al., 1989). Several early experiments have shown that cyclin must accumulate to beyond a critical level in order to trigger mitosis (Evans et al., 1983; Pines and Hunt, 1987; Minshull et al., 1989; Murray and Kirschner, 1989) What is the threshold of cyclin

B protein concentration required to activate MPF? To answer this question, Solomon et al. (1990) added fixed amounts of sea urchin non-degradable cyclin B protein to cycloheximide-treated, CSF-released *Xenopus* egg extracts. The non-degradable cyclin B protein (Δ 87 cyclin B) is missing the degradation box (first 87 amino acids at N terminal), and thus, cannot be degraded by proteolysis. Solomon found 40-50 nM Δ 87 cyclin B protein was required to induce near maximal levels of H1 kinase activity in extracts (Solomon et al., 1990). Solomon also measured a lag time for MPF activation. The lag time is defined *in vivo* as the period before Cdc2 activation occurs during which protein synthesis is no longer required (Wagenaar, 1983; Picard et al., 1985; Karsenti et al., 1987). Thus, even after the threshold concentration of cyclin has been reached, there must be other processes that must be completed before Cdc2 is activated. Solomon et al. found that MPF activation is delayed by 20 minutes *in vitro*, independent of cyclin concentration (Solomon et al., 1990).

However, in Novak and Tyson's model, the lag time is predicted to be dependent on the concentration of cyclin B. When cyclin B concentration is close to the activation threshold, the time required for MPF activation is predicted to become very long (Novak and Tyson, 1993). Jonathan Moore (personal communication) saw a doubling of the lag time for cyclin B concentrations just above threshold. In this study, we measured the activation threshold and lag time to resolve the discrepancy.

1.3.3.2 Inactivation threshold concentration of cyclin B

Supplementation of egg extracts with nondegradable cyclin B1 prevents mitotic exit and causes a stable arrest in late anaphase (Holloway et al., 1993). Stemmann et al. (2001) measured the threshold of cyclin B concentration that inhibits mitotic exit. In Stemmann's experiments, human Δ 87 cyclin B1 protein was added to a CSF-released extract arrested in Mitosis I. The extract was then activated by calcium. They found that mitotic exit was completely inhibited by 40 nM human Δ 87 cyclin B1 protein. However, when cyclin B1 level was 20 nM, the extract exited mitosis (Stemmann et al., 2001). From these data, the inactivation threshold for Mitosis I was determined to be between 20 nM and 40 nM in CSF-released extracts.

In Novak and Tyson's model, the threshold for MPF inactivation (the threshold of cyclin B concentration that inhibits mitotic exit) was predicted to be much lower than the threshold for MPF activation. However, the activation threshold measured by Soloman and the inactivation threshold measured by Stemmann are not directly comparable, since the first one was measured with sea urchin cyclin B expressed in bacteria and the second one was measured with human cyclin B expressed in insect cells. Furthermore, the protein quality varies from prep to prep.

To compare the activation and inactivation thresholds, we returned to these experiments and measured both thresholds by adding human Δ 87 cyclin B1 protein to the same extract at interphase or M phase.

1.3.3.3 Threshold concentration of cyclin B where DNA replication checkpoint is engaged

Using *Xenopus* egg extracts, which spontaneously oscillate between interphase and mitosis, Dasso and Newport found that the onset of mitosis is inhibited by the presence of unreplicated DNA when the concentration of sperm nuclei is 250-300/μl, demonstrating that the completion of DNA replication and the initiation of mitosis are coupled in these extracts (Dasso and Newport 1990). Unreplicated DNA regulates mitosis by promoting tyrosine phosphorylation of Cdc2, thus preventing the full activation of MPF (Dasso et al., 1992). The DNA replication checkpoint can be bypassed by supplementing extracts with constitutively active, nonphosphorylable Cdc2 (Kumagai and Dunphy, 1995). This inhibition can also be overcome by adding Cdc25 protein (Kumagai and Dunphy, 1991; Dasso et al., 1992). A block to mitosis induced by aphidicolin, a DNA polymerase inhibitor, and sufficient sperm nuclei can be released by okadaic acid which inhibits protein phosphatases, resulting phosphorylated and inactive Wee1 and phosphorylated and active Cdc25 (Smythe and Newport, 1992; Izumi et al., 1992). XChk1 is required for the DNA replication checkpoint (Kumagai et al., 1998). XChk1 phosphorylates Cdc25 on Ser-287, which then binds 14-3-3 proteins in the cytocol and inhibits nuclear accumulation of Cdc25 (Kumagai and Dunphy, 1999). XChk1 also phosphorylates

XWee1 on Ser-549, which also binds 14-3-3 proteins, but in this case, in the nucleus. (Lee et al., 2001) Therefore, MPF cannot be activated at DNA replication checkpoint.

As a summary, the current model for DNA replication checkpoint in *Xenopus* egg extract is as follows: unreplicated DNA activates XChk1 which then blocks the activation of Cdc2 by coordinated suppression of Cdc25 and stimulation of Wee1 (Kumagai et al., 1998; Lee et al., 2001).

In Novak and Tyson's model, unreplicated DNA engages a checkpoint by enlarging the hysteresis loop, thereby increasing the activation threshold. The model predicts that high concentration of cyclin B might rescue the extract from the DNA replication checkpoint (Novak and Tyson, 1993). We tested Novak and Tyson's prediction with extracts supplemented with sperm DNA and aphidicolin.

Chapter 2: BISTABILITY and HYSTERESIS

A nonlinear dynamical system controlled by positive feedback may exist in either of two steady states under identical conditions (bistability), depending upon the path by which it arrived at a particular state (hysteresis). Evidence for bistability and hysteresis would indicate that MPF regulation system is a controlled switch-like behavior and is irreversible.

The model of the cell cycle control in *Xenopus* eggs and egg extracts is shown in Fig. 2. Novak and Tyson converted this model into ordinary differential equations (Table 1) and performed numerical simulation for MPF activation and inactivation (Fig. 3).

The model showed that MPF can persist in two alternative states (Fig. 3): an interphase-arrested state with low MPF activity (because Cdc2 is phosphorylated), and an M phase-arrested state with high MPF activity (because Cdc2 is unphosphorylated). The system switches between the two states when the amount of cyclin B in the cell is sufficiently altered. The control system can be induced to jump from one stable steady state to the other by a disturbance large enough to bypass the intervening unstable state. Once it has jumped, the system will remain in its altered state even after removal of the disturbance. To jump back to its original state, the control system must be subjected to a disturbance larger in magnitude and opposite in direction. Thus, hysteretic transitions are irreversible. Novak and Tyson proposed that *Xenopus* egg extracts switch between this two alternative states: interphase and mitosis.

Solomon observed a discrete threshold for MPF activation (local maximum in Fig.3), but did not observe hysteresis (Solomon et al., 1990). If hysteresis is true, there must be another, lower threshold for MPF inactivation which Solomon did not measure (local minimum in Fig.3) (Novak and Tyson, 1993). The difference in thresholds implies that the MPF control system is bistable, which means that between the two thresholds there is a region of alternative stable states with MPF activity either large or small. When the cyclin concentration falls in this region, the extract will remain in interphase if the extract starts from interphase; the extract will remain in M phase if the extract starts from

$$\frac{d[Cyclin]}{dt} = k_1 - k_2[Cyclin] - k_3[Cdk1][Cyclin]$$

$$\frac{d[YT]}{dt} = k_{pp}[MPF] - (k_{wee} + k_{cak} + k_2)[YT] + k_{25}[PYT] + k_3[Cdk1][Cyclin]$$

$$\frac{d[PYT]}{dt} = k_{wee}[YT] - (k_{25} + k_{cak} + k_2)[PYT] + k_{pp}[PYTP]$$

$$\frac{d[PYTP]}{dt} = k_{wee}[MPF] - (k_{pp} + k_{25} + k_2)[PYTP] + k_{cak}[PYT]$$

$$\frac{d[MPF]}{dt} = k_{cak}[YT] - (k_{pp} + k_{wee} + k_2)[MPF] + k_{25}[PYTP]$$

$$\frac{d[Cdc25P]}{dt} = \frac{k_a[MPF]([total\ Cdc25] - [Cdc25P])}{K_a + [total\ Cdc25] - [Cdc25P]} - \frac{k_b[PPase][Cdc25P]}{K_b + [Cdc25P]}$$

$$\frac{d[Wee1P]}{dt} = \frac{k_e[MPF]([total\ Wee1] - [Wee1P])}{K_e + [total\ Wee1] - [Wee1P]} - \frac{k_f[PPase][Wee1P]}{K_f + [Wee1P]}$$

$$\frac{d[IEP]}{dt} = \frac{k_g[MPF]([total\ IE] - [IEP])}{K_g + [total\ IE] - [IEP]} - \frac{k_h[PPase][IEP]}{K_h + [IEP]}$$

$$\frac{d[APC^*]}{dt} = \frac{k_c[IEP]([total\ APC] - [APC^*])}{K_c + [total\ APC] - [APC^*]} - \frac{k_d[Anti\ IE][APC^*]}{K_d + [APC^*]}$$

$$k_{25} = V_{25}'([total\ Cdc25] - [Cdc25P]) + V_{25}''[Cdc25P]$$

$$k_{wee} = V_{wee}'[Wee1P] + V_{wee}''([total\ Wee1] - [Wee1P])$$

$$k_2 = V_2'([total\ APC] - [APC^*]) + V_2''[APC^*]$$

Table 1. Differential equations in Novak-Tyson model (adapted from Fig. 2, Novak and Tyson, 1993, with permission).

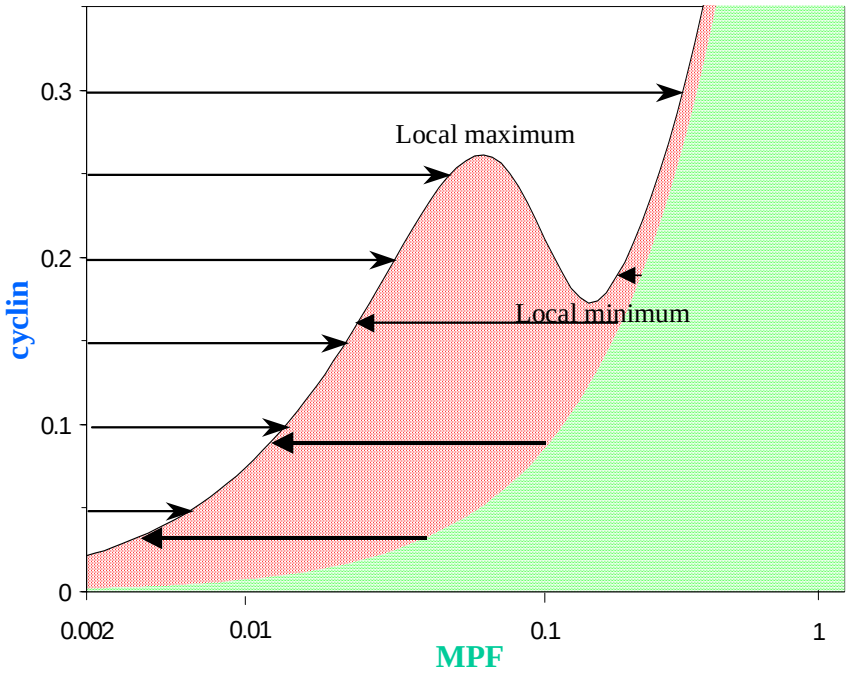

Fig. 3. Prediction 1: The MPF activation threshold concentration of cyclin B is higher than the MPF inactivation threshold concentration of cyclin B (bistability and hysteresis). The N-shaped equilibrium curve implies cyclin thresholds. As cyclin concentration in the extract is increased, there is an abrupt threshold for activation of MPF, given by the local maximum of the dimer equilibrium curve. As cyclin concentration in the extract is decreased, there is a lower threshold for inactivation of MPF, given by the local minimum of the dimer equilibrium curve. (Adapted from Fig. 4B, Novak and Tyson, 1993, with permission.)

M phase. During interphase, cyclin level increases until it rises above the local maximum and MPF become activated. At the completion of mitosis, cyclin degradation is turned on, cyclin level drops below the local minimum, and MPF is inactivated. (Fig. 3)

Novak-Tyson model made three predictions which were tested experimentally in this study to determine if hysteresis underlies MPF regulation in *Xenopus* egg extract:

Prediction 1 (Fig. 3): There should be a threshold for MPF inactivation, if the extract is prepared in the active state. Only when the total cyclin is reduced below this threshold, can MPF be massively inactivated by tyrosine phosphorylation. The cyclin threshold for MPF inactivation, the local minimum of the N-shaped nullcline, should be measurably smaller than the cyclin threshold for MPF activation.

To test prediction 1, three protocols were used. 1) Inactivation threshold for Meiosis II and activation threshold for Mitosis I were compared in CSF-released extract. 2) Inactivation threshold and activation threshold for Mitosis I were compared in cycling extract. 3) Inactivation threshold and activation threshold for Mitosis I were compared in CSF-released extracts.

Prediction 2 (Fig. 4): For cyclin levels just marginally above the activation threshold, there should be a dramatic "slowing-down" in the rate of MPF activation. When the cyclin B level is just greater than the activation threshold, the rate of MPF dephosphorylation is only slightly greater than the rate of MPF phosphorylation, so MPF cannot be activated (dephosphorylated) immediately. Therefore, the "lag" time, from first introduction of exogenous cyclin to the appearance of a significant level of MPF activity, will get longer and longer as the exogenous cyclin level approaches the local maximum of the MPF nullcline (Fig. 3) from above.

To test prediction 2, supra-threshold concentrations of human cyclin B1 Δ87 protein were added to interphase-arrested extract. Lag time for MPF activation was observed by sperm morphology and H1 kinase assay.

Prediction 3 (Fig. 5) : The activation threshold of cyclin B is increased when a DNA replication checkpoint is engaged. Unreplicated DNA causes the local maximum of

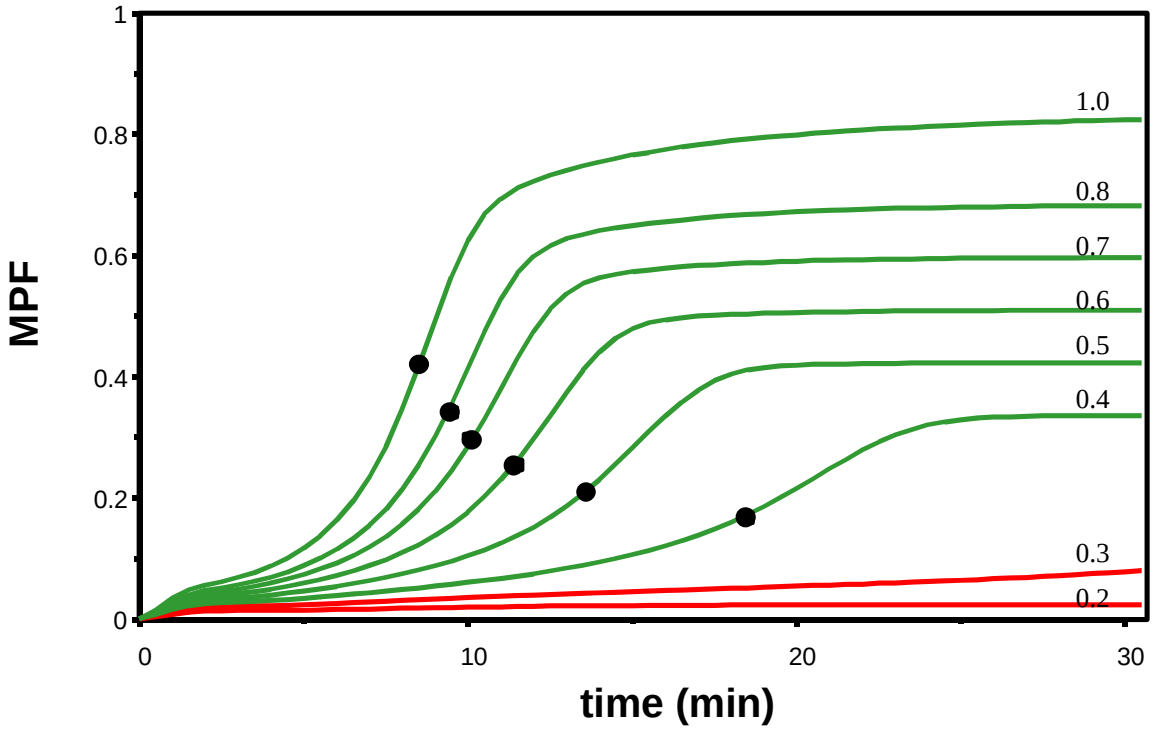

Fig. 4. Prediction 2: As concentration of total cyclin (the values in the right column) drops close to the activation threshold which is 0.2 in this figure, there is a dramatic slowing down (longer lag time) in the rate of MPF activation. The black dots mark the lag point, at 50% of final MPF activity. (Fig. 4A, Novak and Tyson, 1993, with permission)

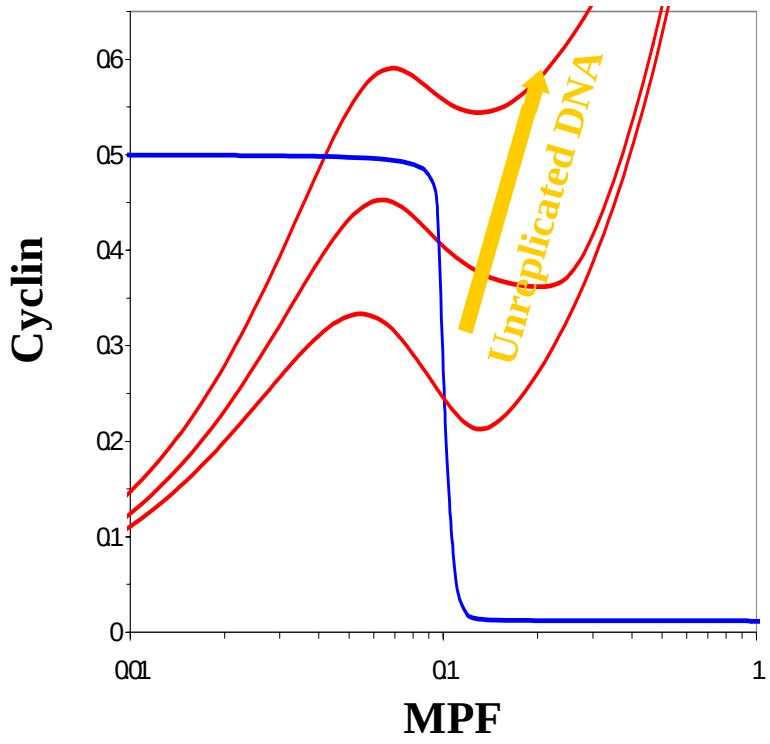

Fig. 5. Prediction 3: Engagement of a DNA replication checkpoint raises the threshold concentration of cyclin required to drive entry into mitosis by increasing the hysteresis loop. (Fig. 5, Novak and Tyson, 1993, with permission.)

the dimer equilibrium curve to increase, so the extract must synthesize more cyclin to activate MPF.

To test prediction 3, known concentrations of human cyclin B1 Δ87 protein were added to the interphase-arrested extract treated with 100 μg/ml aphidicolin and 1200 sperm nuclei/μl.

Chapter 3: MATERIALS and METHODS

3.1 Priming frogs and inducing ovulation

Frogs were injected with 75 U / frog PMSG (pregnant mare serum gonadotropin) on day 1 and were maintained in chlorine-free water at 16°C. These frogs were then injected with 500 U / frog HCG (human chorionic gonadotropin) on day 4 or day 5 and were kept in chlorine-free water with 100 mM NaCl at 23°C. Eggs were collected 14-17 hours after HCG injection.

3.2 Preparation of *Xenopus* egg extracts

3.2.1 CSF extract

Xenopus CSF extracts were prepared essentially as described (Murray et al., 1989).

Laid eggs were collected in 100 mM NaCl, de-jellyed with 2 % (w/v) cysteine in XB salt (0.1 M KCl, 1 mM $MgCl_2$, 0.1 mM $CaCl_2$, pH 7.8) for 5 minutes and washed four times with XB buffer (0.1 M KCl, 1 mM $MgCl_2$, 0.1 mM $CaCl_2$, 10 mM HEPES, 50 mM sucrose, pH 7.7) and then twice with CSF-XB (1X XB buffer plus 5 mM EGTA, pH 7.7, 1 mM $MgCl_2$, 10 μg/ml each of leupeptin, pepstatin and chymostatin). The eggs were then transferred to a centrifuge tube containing 5 ml CSF-XB plus 100 μg/ml cytochalasin B. 1 ml Versilube oil was added to the top of the centrifuge tube to displace excess buffer. The tube was then centrifuged in a table-top centrifuge at 1000 rpm for 60 seconds, then 2000 rpm for 30 seconds. XB buffer was removed from the top of tube. The packed eggs were then centrifuged for 10 minutes at 15,680 g at 4°C (10,000 rpm, JA 13.1 swinging bucket rotor, Beckman). The cytoplasmic fraction was collected and 1/20 volume of CSF energy mix (150 mM creatine phosphate, 20 mM ATP, pH 7.4, 20 mM $MgCl_2$, 200 μg/ml each of leupeptin, chymostatin and pepstatin, 200 μg/ml cytochalasin B) was added. The extract was then centrifuged for 15 minutes at 15,680 g at 2°C (JA 10,000 rpm, 13.1 swinging bucket rotor, Beckman). Sperm nuclei were added to a final concentration of 5×10^5 per ml.

To make interphase-arrested extract from CSF extract, 100 μg/ml cycloheximide was added to CSF extract at 0 minute to block the synthesis of endogenous proteins, then 0.4 mM $CaCl_2$ was added to activate the extract. The extract was then incubated 40 minutes at room temperature to produce the interphase-arrested extract. The protocol is based on the method of Murray et al, (1989).

3.2.2. Cycling extract

Laid eggs were collected in 100 mM NaCl, de-jellyed with 2 % cysteine in XB salt for 5 minutes and washed in 0.2 X MMR (0.02 M NaCl, 0.4 mM KCl, 0.2 mM $MgCl_2$, 0.4 mM $CaCl_2$, 0.02 mM Na_2EGTA and 1 mM HEPES, pH 7.8). To activate eggs, calcium ionophore A23187 (Sigma C-7522) was then added to final concentration of 5 μg/ml. After 60-80 seconds, the eggs were washed 4 times with XB buffer and washed twice with XB buffer plus protease inhibitors (XB buffer + 10 μg/ml each of leupeptin, pepstatin and chymostation). Eggs were then transferred to a centrifuge tube containing XB plus inhibitors and 100 μg/ml cytochalasin B. Versilube oil 1 ml was added to the top of the centrifuge tube to displace excess buffer. The tube was then centrifuged in a table-top centrifuge at 1000 rpm for 60 seconds, then 2000 rpm for 30 seconds. XB buffer was removed from the top of tube. The packed eggs were then centrifuged for 10 minutes at 15,680 g at 2°C (10,000 rpm, JA 13.1 swinging bucket rotor, Beckman). The cytoplasmic fraction was collected and 1/20 volume of energy mix (150 mM creatine phosphate, 20 mM ATP, pH 7.4, 20 mM $MgCl_2$, 2mM EGTA, pH, 7.7, 200 μg/ml each of leupeptin, chymostatin and pepstatin, 200 μg/ml cytochalasin B) was added. The extract was then centrifuged for 15 minutes at 15,680 g at 2°C (10,000 rpm, JA 13.1 swinging bucket rotor, Beckman). Sperm nuclei were added to a final concentration of 5×10^5 per ml. Cycling extract was then released from ice and started the incubation at 23 °C. The time when cycling extract is released from ice is time zero.

To make interphase-arrested extract from cycling extract, 100 μg/ml cycloheximide was added to cycling extract at 0 minutes.

3.3 Expression of recombinant nondegradable human Δ87 cyclin B1 protein

Δ87 cyclin B1 protein is a mutagenically altered form of human cyclin B1 protein that has been truncated via deletion of the first 87 N-terminal amino acids. His-tagged human Δ87 cyclin B1 protein was prepared essentially as described (Kumagai and Dunphy, 1991; Zou et al., 1999). Human cyclin B1 Δ87 baculovirus (originally from Dr. William Dunphy's lab) was provided by Dr. Jonathan Moore, ICRF.

SF9 culture 100 ml at 2×10^6 cells/ml was infected with baculovirus supernatant and harvested after 72-hour incubation at 28°C. The infected cells were centrifuged for 5 minutes at 500 × g at 4°C. Cell pellets from five cultures were equilibrated with 30 ml HBS (10 mM HEPES pH 7.5, 150 mM NaCl, 0.5 mM EGTA, 0.5% (v/v) Triton-X) and resuspended. The cells were lysed by extensive sonication, and the insoluble material was removed by centrifugation for 20 minutes at 15,680 g at 4°C (10,000 rpm, JA 17 swinging bucket rotor, Beckman). The supernatant was applied to a Ni-NTA agarose column. The column was washed with 20 ml HBS containing 20 mM imidazole and 0.5% (v/v) NP-40, then washed with 25 ml HBS. The column was then washed with 1ml HBS containing 200 mM imidazole. The elution was collected in fractions. The Δ87 cyclin B1 was pure as judged by Coomassie blue stained SDS gel. The protein concentration of each fraction was measured by comparing the band density with known concentrations of BSA protein resolved and stained on an SDS gel. Some preparations of Δ87 cyclin B1 were made by Antonio D. Lassaletta.

3.4 Sperm nuclei preparation

The protocol is based on the method of Gurdon (1976).

Four male frogs were injected with 25 U of PMSG 3 days before sperm collection, and then injected with 125 U of HCG the day before collection. The frogs were anesthetized by immersion in ice water for 20 minutes. The testes were removed and rinsed 3 times in cold MMR, then were washed twice in NPB (250 mM sucrose, 15 mM HEPES pH 7.4, 1 mM EDTA pH 8.0, 0.5 mM spermidine trihydrochloride (Sigma), 0.2mM spermine tetrahydrochloride (Sigma), 1mM dithiothreitol (Sigma), 10 μg/ml

leupeptin, 0.3 mM PMSF (Sigma). NPB 2 ml was then added to macerated testes. Testes were then filtered and rinsed with 8ml of NPB and spun down at 3000 rpm for 10 minutes. Sperm were resuspended in 1 ml NPB with 50 μl of 10 mg/ml lysolecithin and incubated for 5 minutes at room temperature. 10ml cold NPB containing 3 % (w/v) BSA was then added. The sperm were centrifuged for 10 minutes at 3000 rpm, resuspended in 5ml NPB containing 0.3% (w/v) BSA and spun down for 10 minutes at 3000 rpm. The sperm were then resuspended in 1ml NPB without PMSF and containing 0.3% (w/v) BSA and 30% (v/v) glycerol. The sperm density was counted with a hemocytometer, adjusted to a final density of 10^7 sperm nuclei/ml, and snap frozen in 25 μl aliquots in liquid nitrogen and stored at –80°C. Sperm nuclei were made by Dr. Katherine Chen.

3.5 Monitoring MPF activity by nuclear morphology

Cell cycle progression was monitored by examining the morphology of sperm nuclei that were fixed and stained with DAPI. 5 μl extract was withdrawn and deposited on a slide, then 5 μl of fix (11.1% (v/v) formaldehyde, 48% (v/v) glycerol, 1 × MMR, 1 μg/ml DAPI (DAPI, Sigma))was added on top of this drop. The slides were viewed under fluorescence and phase contrast microscopy. The sperm morphology for M phase is condensed DNA with no nuclear membrane. The sperm morphology for interphase is decondensed DNA and complete nuclear membrane.

3.6 Monitoring MPF activity by histone H1 kinase assay

H1 kinase activity was assayed by diluting samples tenfold into EB (20 mM HEPES pH7.5, 15 mM $MgCl_2$, 20 mM EGTA, 1 mM DTT, 80 mM β-glycerol phosphate, 0.5 mM PMSF, 3 μg/ml each leupeptin, chymostatin and pepstatin, 50 mM NaF, 1mM $NaVO_4$ and 1 uM microcystin) and assaying for kinase activity by adding 10 μl 2X kinase buffer (containing 1 M HEPES pH 7.5, 1 M $MgCl_2$, 100 mM EGTA, 10 mg/ml BSA, 10 mM ATP, 5 mg/ml calf thymus histone H1, 500 μM PKI (cAMP-dependent protein kinase inhibitor) and 0.5 μCi/μl γ^{32}P ATP) to 10 μl diluted samples. The mixture was incubated at 20°C for 15 minutes. 5X sample dye 5 μl was then added to stop the reaction. The reaction mix was then heated at 80°C for 2 minutes before loading onto a

12.5% (w/v) polyacrylamide gel. The gel was electrophoresed at 35 mA per gel in 1X running buffer (25 mM Tris, 190 mM lycine, 0.1% (w/v) SDS, pH 8.2) for 4 hours. The gel was then stained with Coomassie blue for 1 hour and destained overnight. The amount of incorporated phosphate was detected by autoradiography and quantified by excising the H1 bands and measuring ^{32}P level by Cherenkov scintillation counting.

3.7 Immunoblotting of endogenous cyclin B

Egg extract 1 μl was added into 9 μl EB buffer at indicated timepoints. Samples were snap frozen on dry ice, resolved by 10% (w/v) Laemmli acrylamide gels, transferred to nylon or nitrocellulose membranes, and blotted as described previously (Hartley et al., 1997). The immunoblots were performed by Jill C. Sible and Matthew Petrus.

3.8 Model simulations

All calculations were done on the Novak-Tyson model using parameter values estimated by Marlovits (1998), with two exceptions. 1) According to Fig. 9C, the total Cdc2 pool is close to 80 nM, so we set $[Cdc2]_{total}$=80 nM. 2) values of K_w and K_{25} were reduced 40% (to 1 min^{-1}), because it seems that our cyclin B is not as active as that of Kumagai and Dunphy (1995) upon which the original parameter estimations were based. All the model simulations were done by John Tyson and Chung-Seon Yi.

Chapter 4: RESULTS and DISCUSSIONS

4.1 Prediction 1: the MPF activation threshold concentration of cyclin B is higher than the MPF inactivation threshold concentration of cyclin B.

4.1.1 RESULTS

4.1.1.1 The activation threshold for Mitosis I is higher than the inactivation threshold for Meiosis II in CSF-released extract. (Fig. 6)

Experimental design is shown in Fig. 6A.

CSF extract was supplemented with 500 sperm nuclei per μl. To measure the activation threshold for Mitosis I, cycloheximide was added to CSF-released extract at 0 minutes. The time that CSF extract was released by calcium is time zero. Known concentrations of Δ87 cyclin B protein were added to the cycloheximide-treated, CSF-released extract at 50 minutes when the extract was in interphase. Samples were taken at 120 minutes. The extract to which 32 nM Δ87 cyclin B protein was added remained in interphase. By contrast, extracts to which 40 nM and 60 nM Δ87 cyclin B protein were added entered Mitosis I. From these observations, the activation threshold was inferred to be between 32 nM and 40 nM (Fig. 6B (a)).

The inactivation threshold for Meiosis II was also measured in the same extract. Known concentrations of Δ87 cyclin B1 protein were added to cycloheximide-treated CSF-released extract at 0 minutes. Samples were collected for sperm morphology at 50 minutes. As shown is Fig. 6B (b), extract supplemented with 24 nM Δ87 cyclin B1 exited from in Meiosis II. Extracts supplemented with 32 nM, 40 nM and 60 nM Δ87 cyclin B1 arrested in Meiosis II at 50 minutes. Extracts were monitored for up to 70 minutes with no further detectable changes in sperm morphology (data not shown). From these data, the inactivation threshold for Meiosis II lies between 24 nM and 32 nM.

In this experiment, the cyclin B level that was required to activate MPF was higher than the cyclin B level that was required to inactivate MPF. Extracts supplemented with an intermediate concentration of 32 nM cyclin B remained in M-phase when the protein

was added during meiosis, and remained in interphase when the protein was added during interphase.

To verify that cycloheximide inhibits synthesis of endogenous cyclins in this experiment, the level of endogenous cyclin B1 was monitored by immunoblot samples of the CSF-released extract and the cycloheximide-treated, CSF-released extract. As shown in Fig. 6C, cycloheximide completely inhibited endogenous cyclin B1 synthesis. Thus, the activation and inactivation thresholds are completely determined by exogenous cyclin B1 protein concentration.

In this experiment, the activation threshold and the inactivation threshold were tested on different M phases, Meiosis II and Mitosis I. The fundamental difference between meiosis and mitosis could account for different thresholds. To measure the activation and inactivation thresholds in a more comparable context, we next measured the activation and inactivation thresholds on the same M phase, Mitosis I.

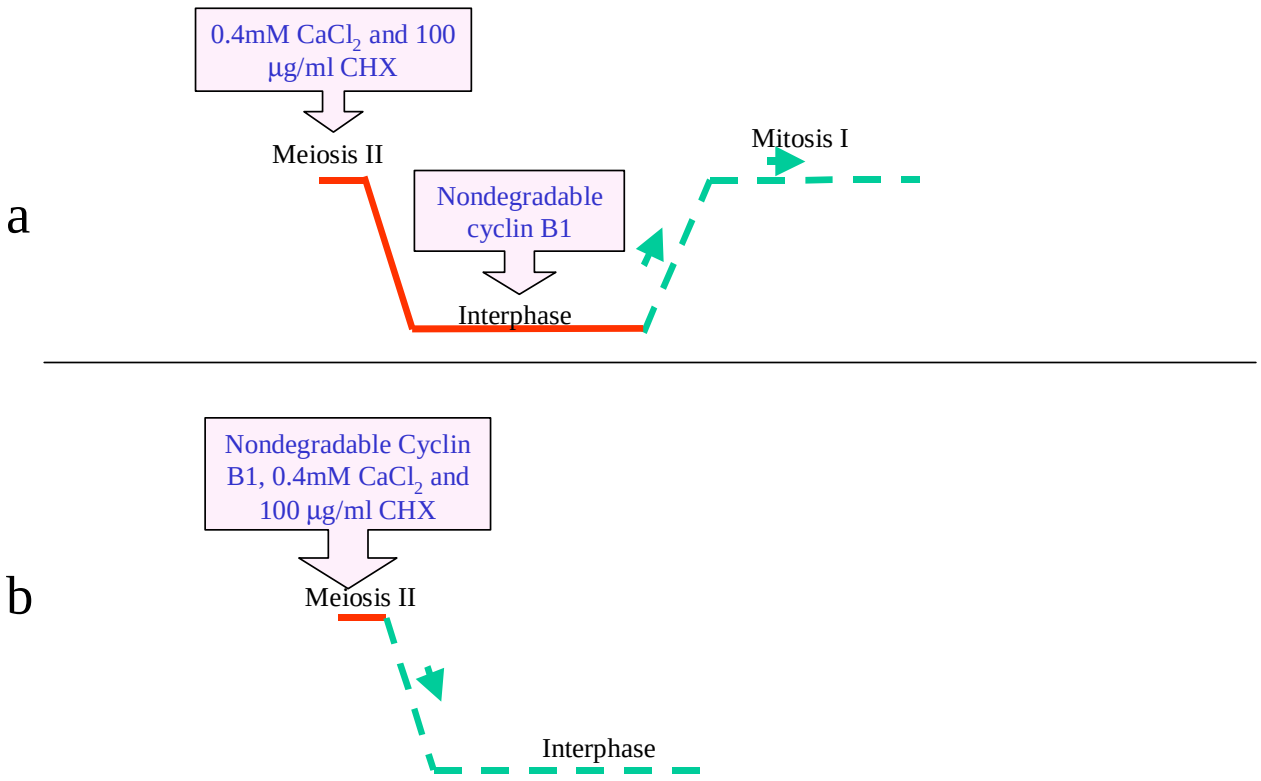

Fig. 6A. Experimental design for comparing activation threshold of Mitosis I and inactivation threshold of Meiosis II in CSF-released extract. a) To measure the activation threshold for Mitosis I, 100 µg/ml cycloheximide was added to CSF released extract at 0 minutes. Δ87 cyclin B1 at different concentrations were added to this extract when it entered interphase. b) To measure the inactivation threshold for Meiosis II, 100 µg/ml cycloheximide and different concentrations of Δ87 cyclin B1 were added to CSF released extract at 0 minutes. The time of calcium addition = time zero.

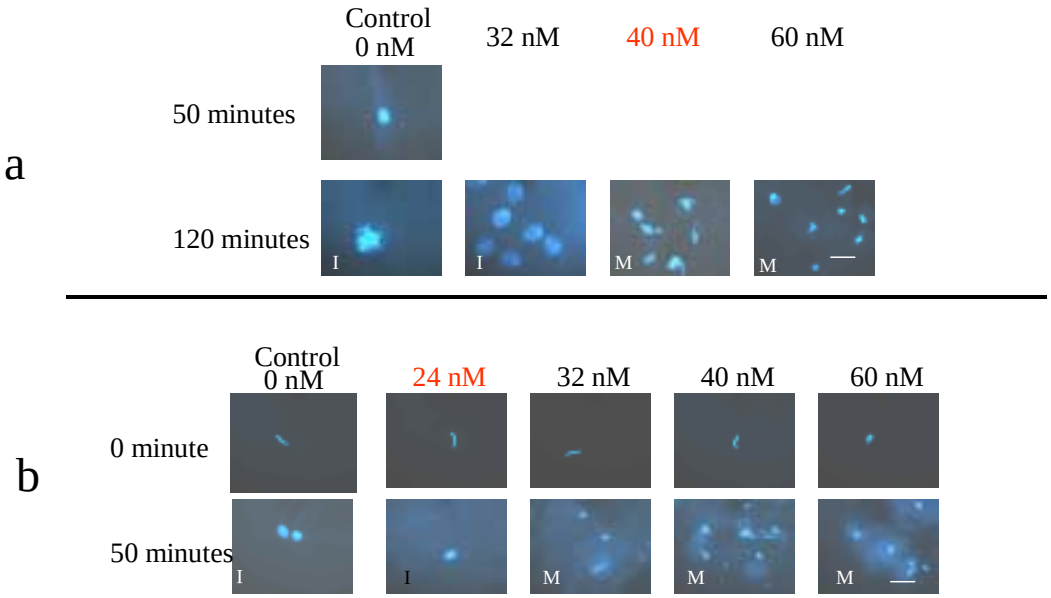

Fig. 6B. The activation threshold for Mitosis I is higher than the inactivation threshold for Meiosis II. Experiment was performed as described in Fig. 6A. Nuclei were photographed by fluorescence microscopy which shows DNA bound by DAPI (a DNA-binding dye). a) To test the activation threshold, Δ87 cyclin B1 protein was added to cycloheximide-treated CSF-released extract at 50 minutes (when extract was in interphase). Nuclei were photographed at 120 minutes. b) To test the inactivation threshold, Δ87 cyclin B1 protein was added to cycloheximide-treated CSF-released extract at 0 minutes (when extract was in Meiosis II). Nuclei were photographed at 50 minutes. Both thresholds were measured in the same extract preparation. I = interphase; M = M phase. Extracts are labelled M when >90% nuclei on slide appear mitotic (condensed chromatin and no nuclear envelope). Scale bar = 50 μm.

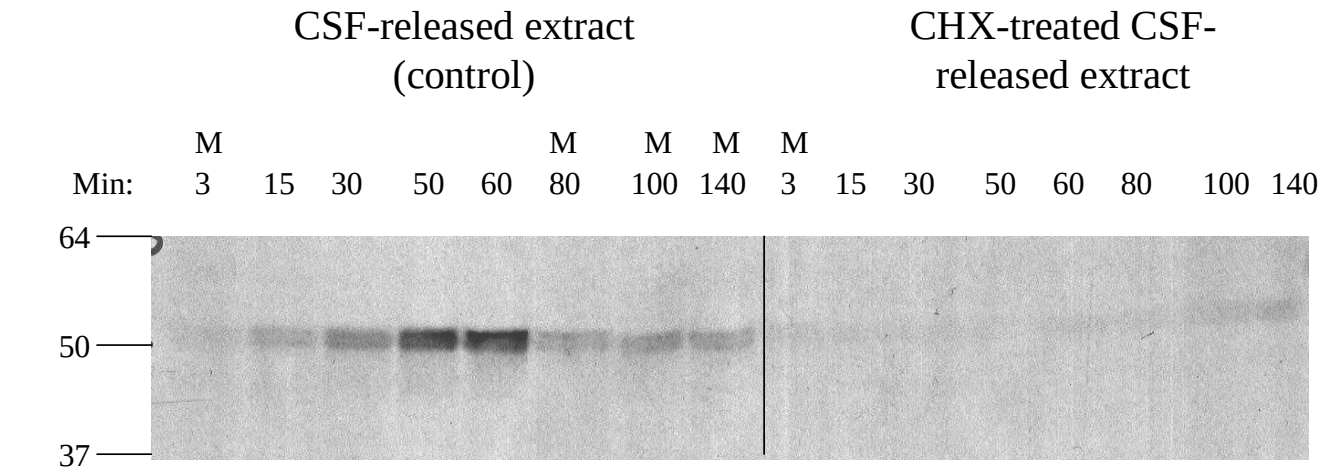

Fig. 6C. Immunoblot for endogenous cyclin B1 protein in CSF-released extract prepared as in Fig. 6B. CHX= cycloheximide. (Performed by Jill Sible).

4.1.1.2 Activation threshold for Mitosis I is higher than inactivation threshold for Mitosis I in cycling extract (Fig. 7)

Experimental design is shown in Fig. 7A.

Cycling extract was supplemented with 500 sperm nuclei per μl. To measure the activation threshold for Mitosis I (Fig. 7Ba), this extract was split into five tubes. Each of them was supplemented with 100 μg/ml cycloheximide and different concentrations of human nondegradable cyclin B1 (Δ87 cyclin B1) protein. The extracts were incubated at 23°C. The time that cycling extract was released from ice and started the incubation at 23°C is time zero. At 90 minutes, the extract containing 40 nM Δ87 cyclin B1 protein had already entered Mitosis I. However, the extracts containing 0 nM, 16 nM, 24 nM and 32 nM Δ87 cyclin B1 had arrested in interphase. Thus, the activation threshold was inferred to be between 32 nM and 40 nM.

To measure the inactivation threshold for Mitosis I (Fig. 7Bb), cycling extract was split into five tubes. Each of them was supplemented with different concentrations of human Δ87 cyclin B1 protein. These extracts were then incubated at 23°C at 0 minutes. At 60 minutes, all of the extracts were in Mitosis I. At 100 minutes, only the extract with no added Δ87 cyclin B1 exited Mitosis I. At 140 minutes, the extracts containing 0 nM and 16 nM Δ87 cyclin B1 protein had both entered interphase. However, the extracts containing 24 nM, 32 nM and 40 nM Δ87 cyclin B1 protein were still arrested at Mitosis I. Therefore, the inactivation threshold for Mitosis I in cyclin extract was between 16 nM and 24 nM.

To measure MPF activity quantitatively, samples taken from the extracts prepared as above were analyzed by H1 kinase assay (Fig. 7C). This assay correlated well with sperm morphology and numerical simulations of the mathematical model (Fig. 7C). As shown in Fig. 7C, at 90 minutes, all cycloheximide–treated extracts displayed low MPF activity except those supplemented with 60 nM Δ87 cyclin B1. At 140 minutes, MPF activity was low in samples that exited mitosis (0-12 nM Δ87 cyclin B1), but higher in

samples that remained in mitosis (24-60 nM Δ87 cyclin B1). MPF activity was proportional to the concentration of Δ87 cyclin B1 above the inactivation threshold, in agreement with numerical simulations (Fig. 7C).

To verify that endogenous cyclin B synthesis was inhibited by cycloheximide, cyclin B1 protein was immunoblotted in these extracts. As shown in Fig. 7D, cycloheximide completely inhibited cyclin B1 synthesis during both interphase I and interphase II. Similar results were obtained when blots were probed for Cyclin B2 (data not shown). Without endogenous cyclin B, MPF activation and inactivation thresholds are only determined by exogenous cyclin B protein concentration in these extracts.

From this set of data, the activation threshold for Mitosis I is higher than the inactivation threshold for Mitosis I in cycling extracts. Intermediate concentrations of 24 nM and 32 nM could support either interphase or mitosis, depending on starting conditions, confirming bistability and hysteresis in MPF regulation system. This result is similar to the result in Fig. 6 which compared meiotic exit and mitotic entry.

Therefore, the protocols in Fig. 6 and Fig. 7 both confirmed bistability and hysteresis.

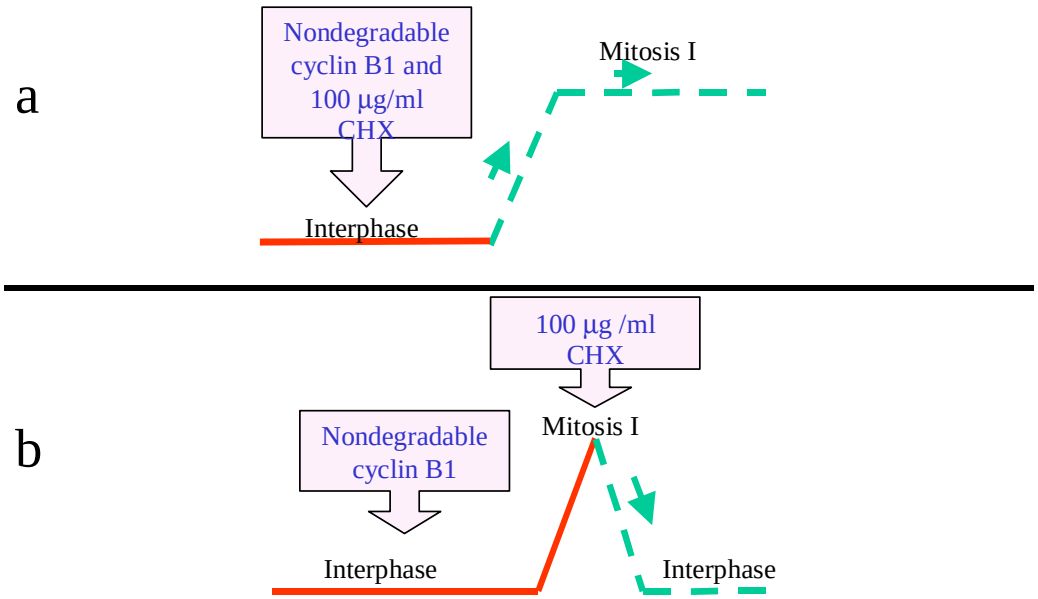

Fig. 7A. Experimental design for comparing activation and inactivation thresholds for Mitosis I in cycling extract. a) To test the activation threshold, 100 µg/ml cycloheximide and different concentrations of Δ87 cyclin B1 protein were added to cycling extract at 0 minutes. b) To test the inactivation threshold, different concentrations of Δ87 cyclin B1 protein were added to cycling extracts. Cycloheximide was added to these extracts when they entered Mitosis. Time zero = the time when cycling extract is released from ice.

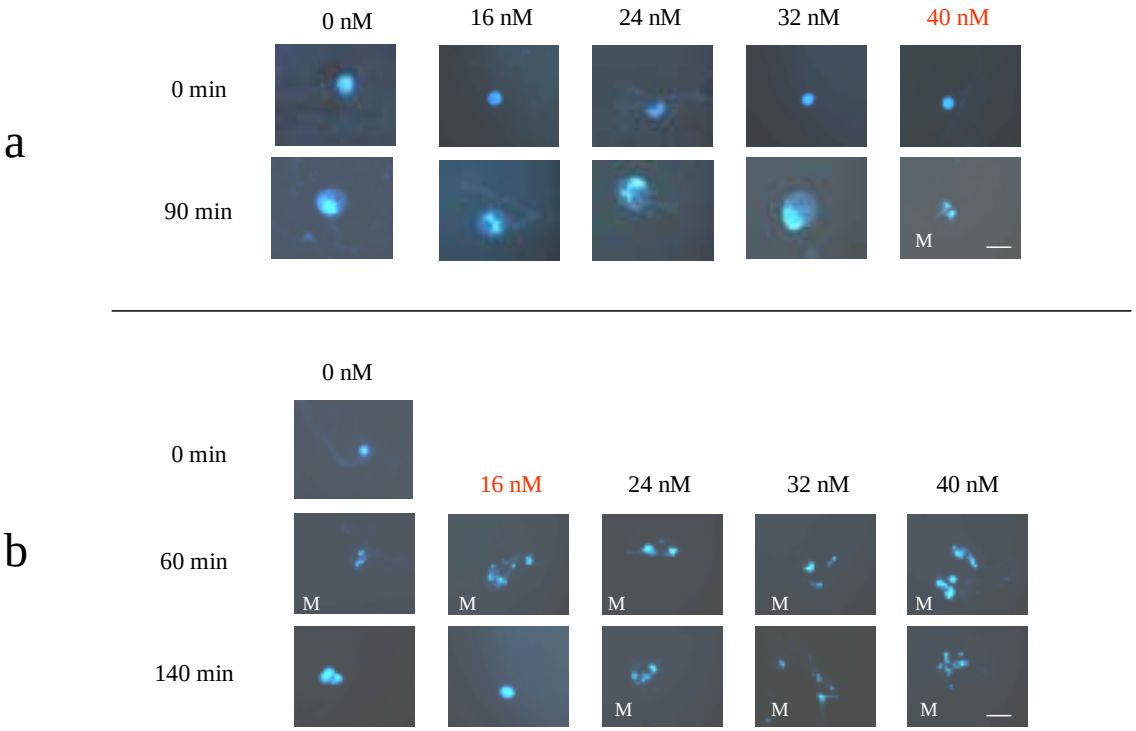

Fig. 7B. The activation threshold for Mitosis I is higher than the inactivation threshold for Mitosis I in cycling extract. Nuclei were photographed by fluorescence microscopy. Experiment was performed as described in Fig. 7A. a) To test the activation threshold, Δ87 cyclin B1 protein was added to cycloheximide-treated cycling extracts at 0 minutes (when extract was in interphase). Nuclei were photographed at 90 minutes. b) To test the inactivation threshold, Δ87 cyclin B1 protein was added to cycling extracts at 0 minutes (when extract was in interphase). Cycloheximide was added to these extracts when it entered Mitosis I at 60 mintutes. Nuclei were photographed at 140 minutes. Both thresholds were measured in the same extract preparation. M = mitosis. Extracts are labelled M when >90% nuclei on slide appear mitotic (condensed chromatin and no nuclear envelope). Scale bar = 50 μm.

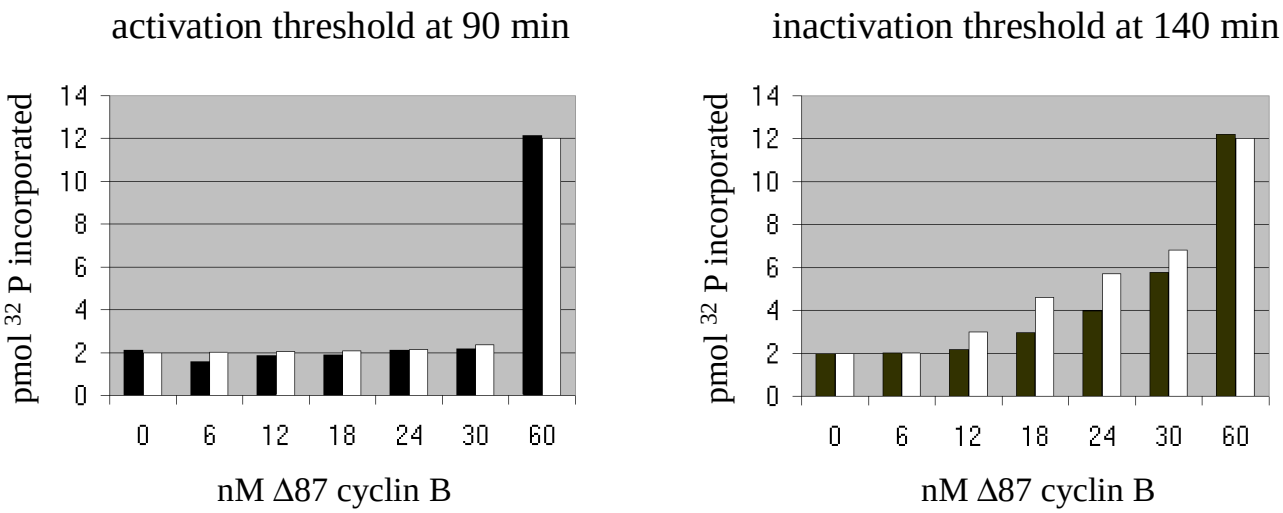

Fig. 7C. H1 kinase assay and model simulations. Samples from extracts as prepared in 7B were analyzed by H1 kinase assay. Experimental data (black bars) are compared to numerical simulations (white bars) of the Novak-Tyson model. (Model simulation was done by John Tyson and Chung-Seon Yi).

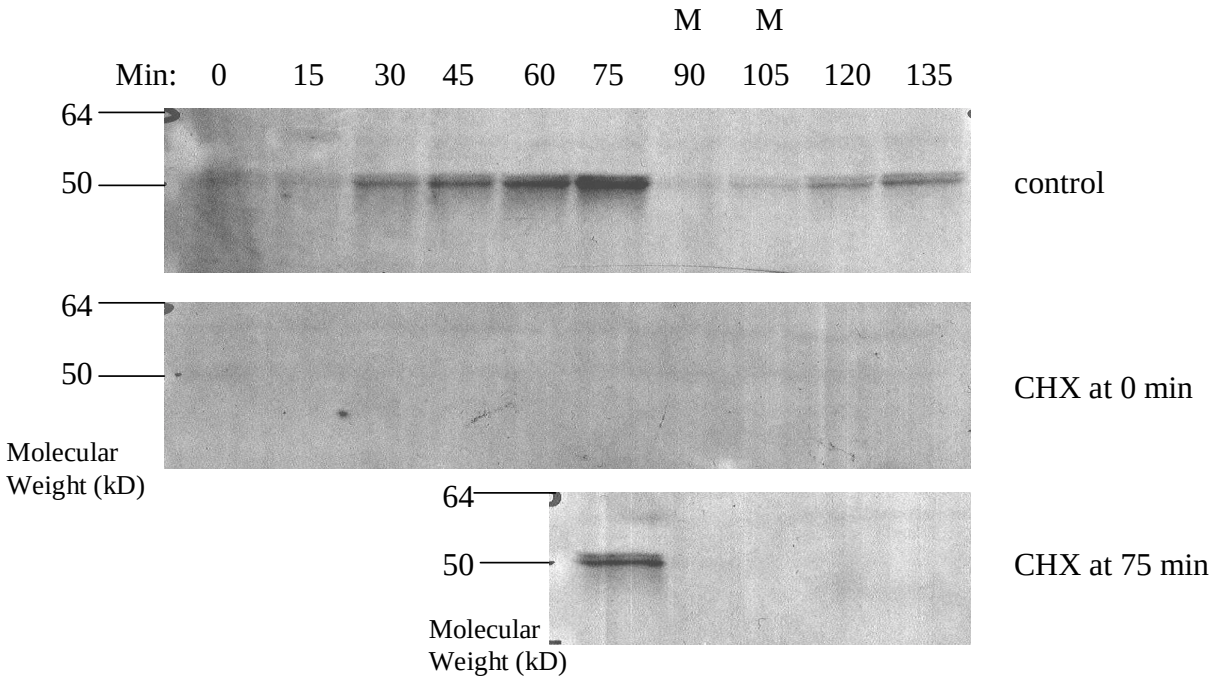

Fig. 7D. Immunoblot for endogenous cyclin B1 in cycling extract prepared as in 7B. CHX= cycloheximide. (Performed by Jill Sible).

4.1.1.3 Different activation and inactivation thresholds for Mitosis I were not detected in CSF extract released with high calcium. (Fig. 8)

Activation and inactivation thresholds for Mitosis I were also measured in CSF-released extracts. The experimental design is shown in Fig. 8A. CSF-released extract can cycle through Meiosis II, interphase, Mitosis I and usually arrest at Mitosis I. Murray suggested Mitosis I arrest in CSF extract is caused by the reactivation of CSF (Murray, 1991). Calcium addition to CSF extract at Mitosis I can be used to release CSF extract from Mitosis I (Holloway et al., 1993; Stemmann et al., 2001). In this experiment, high calcium (0.60 mM) was added at time zero to induce a CSF extract to cycle past Mitosis I.

CSF extract was supplemented with 500 sperm nuclei per μl.

To measure the activation threshold for Mitosis I (Fig. 8Ba), 0.60 mM $CaCl_2$ was added to CSF extract for activation (= time zero). Cycloheximide was added to this CSF-released extract at 0 minutes. Known concentrations of human Δ87 cyclin B protein were added to this extract at 40 minutes (interphase). Samples were removed at 90 and 120 minutes for analysis of sperm morphology. When exogenous cyclin B level was 32 nM or higher, the extracts entered Mitosis I; when cyclin B concentration was 24 nM or lower, the extracts remained in interphase at 120 minutes. Extracts were monitored up to 160 minutes with no further change in sperm morphology. Thus, the activation threshold is between 24 nM and 32 nM.

To measure the inactivation threshold for Mitosis I (Fig. 8Bb), the same CSF extract preparation was activated by adding 0.60 mM $CaCl_2$ and cycled through interphase. The extract was then split into different tubes. Known concentrations of human Δ87 cyclin B protein were added to these extracts at 40 minutes (interphase). All of these extracts entered Mitosis I at 90 minutes. Cycloheximide was added to this extract at Mitosis I to prevent further endogenous protein synthesis. Extracts containing 32 nM or higher concentrations of Δ87 cyclin B remained in Mitosis I at 160 minutes. In

contrast, extracts containing 24 nM or lower concentration of Δ87 cyclin B exited Mitosis I. These results showed that the inactivation threshold lies between 24 nM and 32 nM.

The inactivation threshold was first measured with the same protocol by Stemmann et al. by adding human Δ87 cyclin B1 in a CSF-released extract (Stemmann et al., 2001). The inactivation threshold for Mitosis I was found to be 40 nM, very close to the threshold that we measured.

This experiment showed identical activation and inactivation thresholds, which is inconsistent with thresholds measured by cycling extract and the thresholds measured by CSF extract activated by lower calcium concentration.

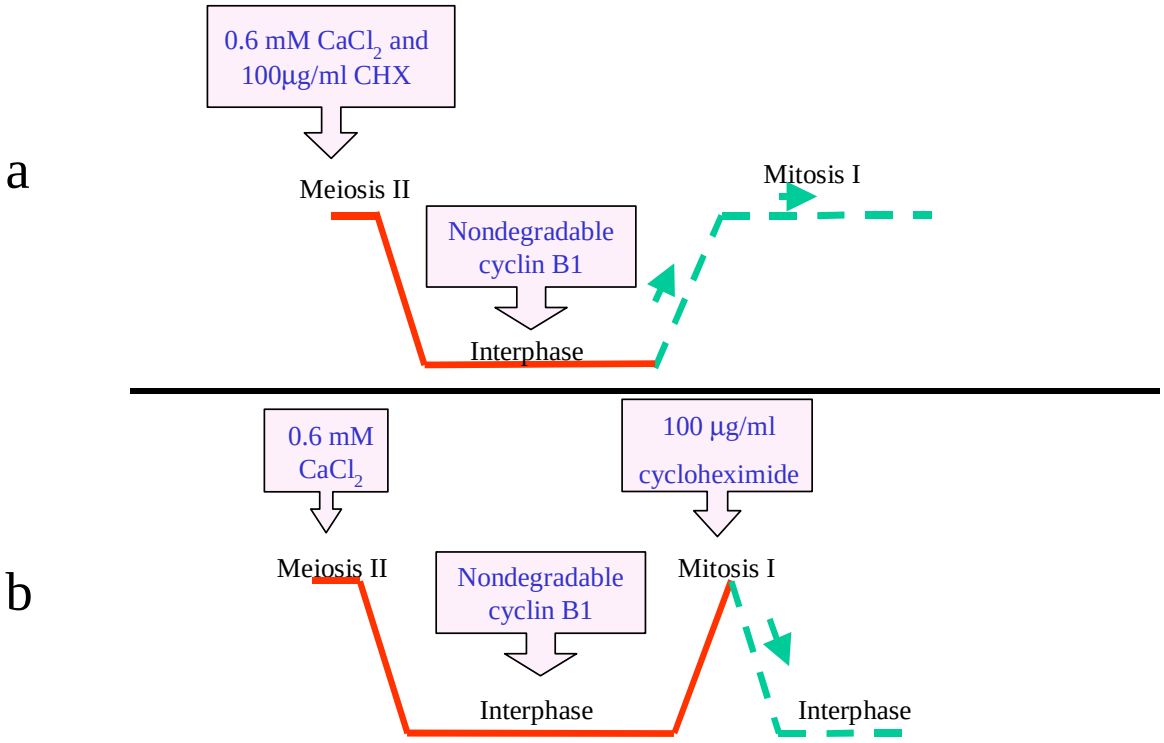

Fig. 8A. Experimental design for comparing activation and inactivation thresholds of Mitosis I in CSF-released extract. a) To test the activation threshold, 100 µg/ml cycloheximide was added to CSF-released extract, different concentrations of Δ87 cyclin B1 protein were added to this extract when it entered interphase. b) To test the inactivation threshold, different concentrations of Δ87 cyclin B1 protein were added to CSF-released extract when it entered interphase. Cycloheximide was added to this extract when it entered Mitosis I.

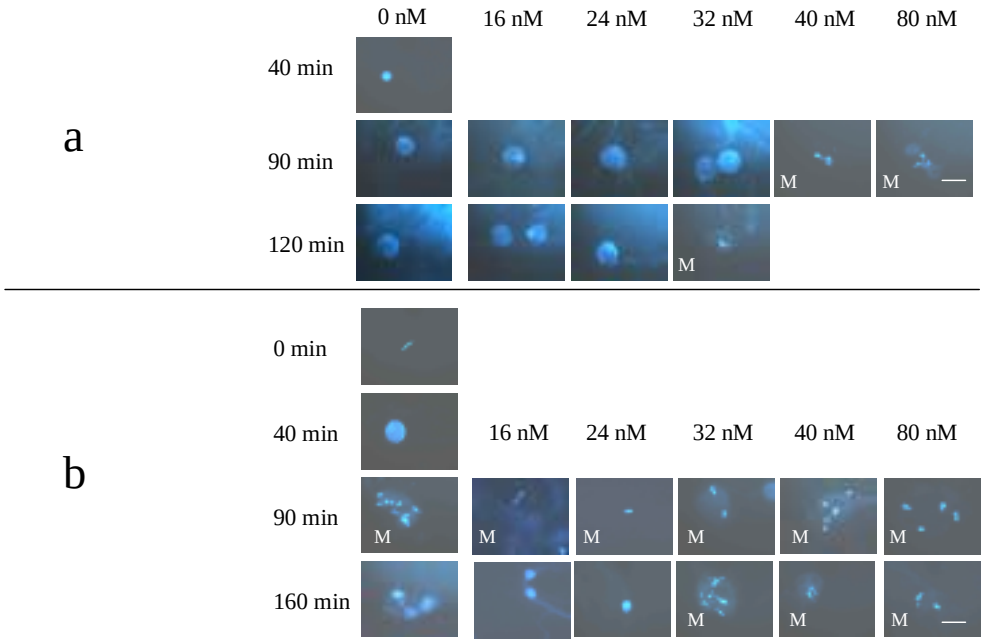

Fig. 8B. The activation and inactivation thresholds for Mitosis I were indistinguishable in CSF-released extract. Sperm nuclei were photographed by fluorescence microscopy. Experiment was performed as described in Fig. 8A. a) To test the activation threshold, Δ87 cyclin B1 protein was added to cycloheximide-treated, CSF-released extracts at 40 minutes (when extract was in interphase). Nuclei were photographed at 90 and 120 minutes. b) To test the inactivation threshold, Δ87 cyclin B1 protein was added to CSF-released extracts at 40 minutes (when extract was in interphase). Cycloheximide was added to these extracts when it entered Mitosis I at 90 mintutes. Nuclei were photographed at 160 minutes. Both thresholds were measured in the same extract preparation. M = M phase. Extracts are labelled M when >90% nuclei on slide appear mitotic (condensed chromatin and no nuclear envelope). Scale bar = 50 μm.

4.1.2 DISCUSSION

In Novak-Tyson's mathematical model (1993), interphase and M phase are two self-maintaining states of the cell cycle. If the extract starts from interphase, MPF cannot be activated and the extract cannot enter M phase until the cyclin B protein level accumulates to the activation threshold to initiate the positive feedbacks. In these positive feedback loops, MPF activates Cdc25 and inactivates Wee1, which further dephosphorylate and activate pre-MPF. If the extract starts from Mitosis, negative feedback triggers cyclin B degradation, but MPF cannot get inactivated, and this extract cannot exit M phase until the total cyclin B level decreases to the inactivation threshold at which point the positive feedbacks are turned off. For activation, the extract starts from a stable steady state where MPF activity is low, and the positive feedbacks are off, which keeps pre-MPF inactive. For inactivation, the extract starts from a stable steady state where MPF activity is high. The positive feedbacks are already on, which keeps MPF activated. The activation threshold is higher than the inactivation threshold, because the extracts start from different stable steady states with positive feedbacks either off or on. Thus, MPF activity is not only dependent on cyclin B protein concentration, but also dependent on the starting state (interphase or M phase). Hysteresis occurs in systems with multiple steady states and refers to the fact that the observed state of the system depends not only on its parameter values but also on its history (how the system is prepared) (Novak et al., 1998).

In our studies, different thresholds (hysteresis) were observed by comparing the inactivation threshold for Meiosis II with the activation threshold for Mitosis I in CSF-released extract (Fig. 6) and by comparing the inactivation threshold for Mitosis I with the activation threshold for Mitosis I in cycling extract (Fig. 7). Thus, we confirmed hysteresis and bistability in two different protocols (Fig. 6 and Fig. 7). However, the different thresholds were not detected in CSF extract released with high calcium concentration (Fig. 8).

Calcium can facilitate both MPF activation and inactivation (Beckhelling et al., 2000). In *Xenopus* egg extracts, addition of calcium chelators could block either activation or inactivation of MPF, depending on the concentration used and the time of addition. Inhibition was achieved without significant reduction in the global free calcium level, which remained in the physiological range (around 200 nM) (Lindsay et al., 1995; Beckhelling et al., 1999).

The mechanism of how calcium triggers mitotic entry and exit (MPF activation and inactivation) remains unclear. Released calcium may act co-operatively with localized MPF regulatory molecules to trigger both mitotic entry and exit (Beckhelling et al., 2000). To facilitate mitotic entry, local intracellular calcium release may stimulate MPF activation via Cdc25/Myt1 regulation of Cdc2 phosphorylation. CaM kinase II, a target of calcium-calmodulin, is a key sensor of calcium transient in cell cycle transitions, including mitotic entry (Baitinger et al., 1990; Santella, 1998). This kinase has been shown to phosphorylate and increase the activity of human Cdc25 in vitro (Patel et al., 1999). To facilitate mitotic exit, calcium signal is involved in MPF inactivation by activating CaM kinase II which eventually triggers cyclin degradation (Lorca et al., 1993). Beckhelling et al. suggested a calcium transient marks the end of the protein synthesis requirement for mitosis by triggering the MPF autoamplification loop (positive feedback loop). When MPF has activated, the elevated MPF activity, together with a further transient calcium increase provides appropriate conditions for activating the anaphase promoting complex, thereby triggering mitotic exit (Beckhelling et al., 1999). Therefore, a possible explanation for the identical thresholds in CSF extract containing high calcium is that high calcium may decrease the activation threshold and increase the inactivation threshold by facilitating both activation and inactivation.

This hypothesis needs to be tested in the future by measuring and comparing both activation and inactivation thresholds in the extracts with different calcium concentrations. Future work is required to unravel the complex relationships between intracellular calcium regulation, CSF activity and enzymatic feedback loops for a complete understanding of the regulation of mitosis.

4.2 Prediction 2: A dramatic "slowing down" in the rate of MPF activation at concentrations of cyclin B marginally above the activation threshold.

4.2.1 RESULTS (Fig. 9)

In Novak and Tyson's model, when cyclin B level is just above the threshold, the system passes just above the dimer equilibrium curve, and, as it does so, the velocity of its motion becomes very slow because the equilibrium curve is a locus of states for which the net rate of dimer transformations is identically zero. Thus, Novak and Tyson predicted: The lag time for cyclin-induced MPF activation should increase dramatically as cyclin approaches the threshold level from above. This effect has not been described in other literature.

This prediction was tested in CSF-released extract. Experimental design is shown in Fig. 9A.

CSF extract was supplemented with 500 sperm nuclei per μl.

As shown in Fig. 9B, known concentrations of nondegradable human cyclin B1 protein were added to 100 μg/ml cycloheximide-treated, CSF-released extract at 30 minutes (interphase). Samples were taken every 15 minutes after protein addition. Sperm nuclei morphology is shown in Fig. 9B. When the cyclin B1 protein concentration was close to the threshold, 40 nM, the time for MPF activation was between 45 minutes and 60 minutes. When the cyclin B1 protein was 50 nM, the lag time was between 30 and 45 minutes. When the cyclin B1 protein was 60 nM, 80 nM or 400 nM, the lag time was between 20 minutes and 30 minutes. Clearly, there was a distinct "slowing down" of the MPF activation process as the cyclin threshold was approached from above, exactly as predicted by the model. H1 kinase assay (Fig. 9C) shows the same result as sperm nuclei morphology (Fig. 9B). Numerical simulation of the model (Fig. 9D) was done and was compared to experimental data. The excellent agreement of the model to the data confirms the accuracy of rate constants estimated for the model (Marlovits, 1998).

4.2.2 DISCUSSION

In 1990, Solomon et al. found the lag time for activation of MPF by exogenous cyclin B in *Xenopus* egg extract was independent of cyclin B concentration. The concentrations that were used in their experiment were: 32 nM, 100 nM, 320 nM and 1000 nM (Fig.3, Solomon et al., 1990). Solomon reported the lag time was 20 minutes at each of these concentrations. There might be two reasons contributing to the discrepancy between his data and our data: 1) we used both sperm morphology and H1 kinase assay to measure MPF activity; Solomon only used H1 kinase assay to measure MPF activity. In our H1 kinase assay, we did see some kinase activities 30 minutes and 45 minutes after low concentration (40 nM) cyclin B was added, but these kinase activities were much lower than the kinase activity for 60nM, 80 nM and 400 nM at the same timepoints. The kinase activities for 40 nM cyclin B at 30 and 45 minutes were not enough for sperm nuclei condensation and nuclear membrane breakdown. Therefore, the lag time for 40 nM was not 30 minutes or 45 minutes, but actually 60 minutes when mitotic nuclei were observed. Solomon did not test sperm morphology, so the lag time might be interpreted differently. In their experiment, the kinase activity at 32 nM was apparently lower than the kinase activity for other high cyclin concentrations. If sperm morphology was assessed, this kinase activity might not be enough for mitosis. Thus, 32 nM may either lower than the threshold or just above the threshold with a longer lag time. If a longer time could have been waited for measuring MPF activity in their experiment, they may see higher kinase activity. 2) It makes sense that the lag time for 100 nM, 320 nM and 1000 nM were the same in their experiment, because all of these concentrations are much higher than the activation threshold. The lag time for these high concentrations should be approximately equal to the minimum lag time, because the positive feedbacks were engaged at these high concentrations. In our experiment, the lag times for 60 nM, 80 nM and 400 nM were all 20 to 30 minutes, which is the minimum lag under our experimental conditions.

We also noticed that the kinase activity for 80 nM is almost the same as the kinase activity for 400 nM, which indicates that the endogenous pool of Cdc2 is close to 80 nM. This measurement is consistent with Solomon's result (Solomon et al., 1990).

From this set of data, we conclude that Novak-Tyson's prediction about the lag time is accurate. There is a dramatic "slowing down" of the MPF activation when cyclin B protein concentration is close to the activation threshold from above.

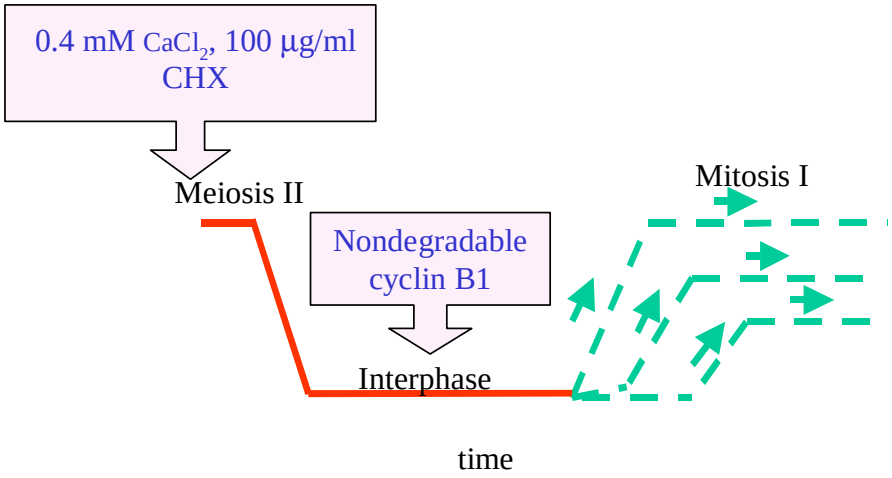

Fig. 9A. Experimental design for measuring the lag time. Different concentrations of Δ87 cyclin B1 protein were added to 100 µg/ml cycloheximide treated CSF-released extract. Samples were collected every 15 minutes for microscopic analysis of nuclear morphology and histone H1 kinase activity.

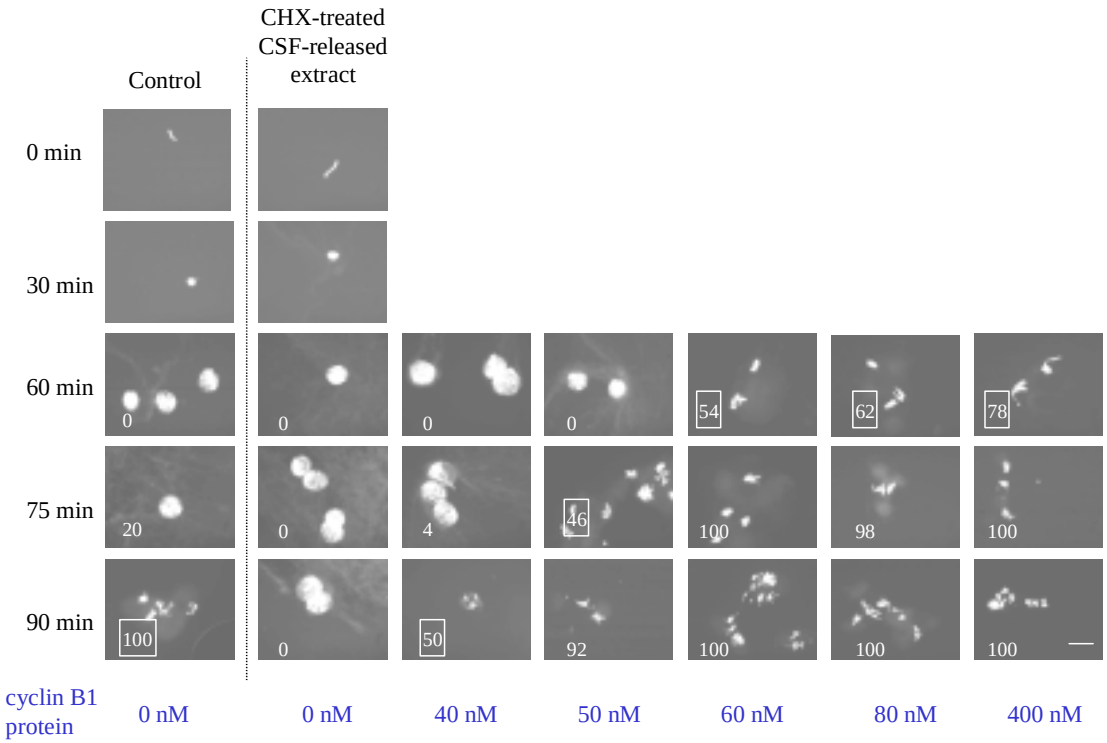

Fig. 9B. MPF activation exhibits a "critical slowing down" near the activation threshold concentration of cyclin B. Experiment was performed as described in Fig. 9A. Δ87 cyclin B1 protein was added to cycloheximide-treated CSF-released extract at 30 minutes when this extract was in interphase. Samples were taken at indicated timepoints for fluorescence microscopy. The extract was qualitatively scored as entering mitosis (boxed numbers) when >40% of the nuclei were in mitosis. Scale bar = 50 μm.

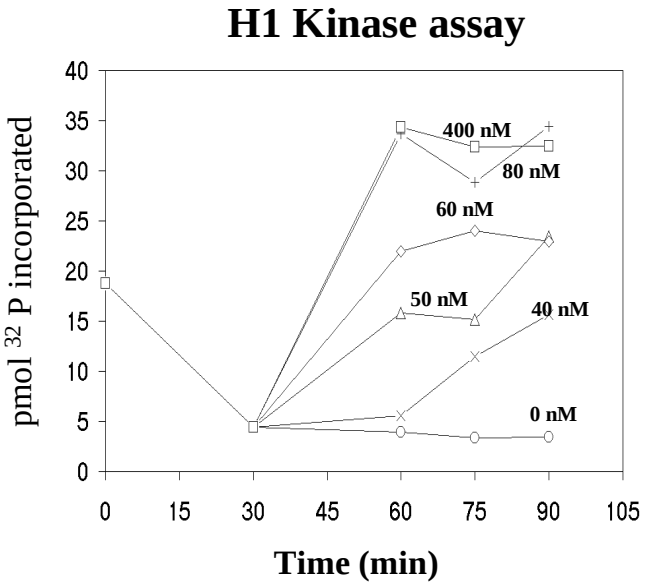

Fig. 9C. H1 kinase assay for the extract in Fig. 9B.

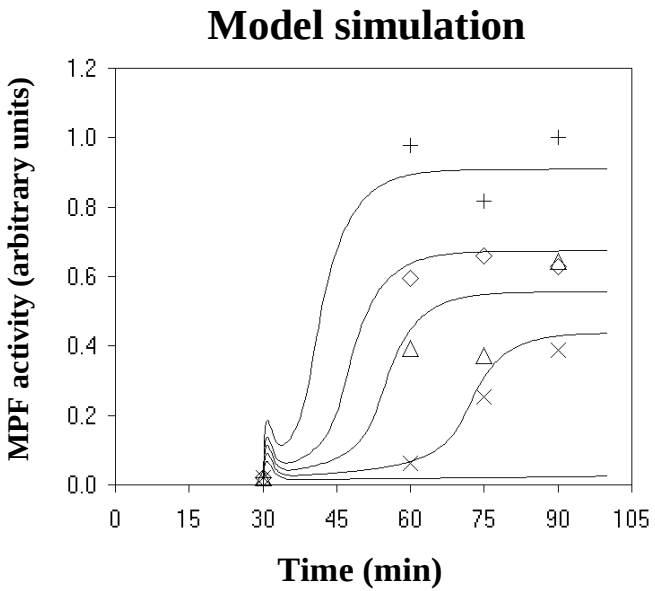

Fig. 9D. Model simulations for the extract in Fig. 9B. Experimental data from 9C (symbols) are displayed alongside simulaions of Novak-Tyson model (curves) (simulated by John Tyson and Chung-Seon Yi)

4.3 Prediction 3: The activation threshold is increased when the DNA replication checkpoint is engaged.

4.3.1 RESULTS (Fig. 10)

Based on some early experimental data, Novak and Tyson predicted a higher activation threshold concentration of cyclin B when a DNA replication checkpoint is engaged (Fig. 5) (Novak and Tyson, 1993). To measure the activation threshold at the DNA replication checkpoint, we added known concentrations of human Δ87 cyclin B to aphidicolin and cycloheximide-treated, interphase-arrested extract. Experimental design is shown in Fig. 10A.

To trigger a DNA replication checkpoint, there must be enough unreplicated DNA. In 1989, Newport and Dasso successfully made a DNA replication checkpoint in *Xenopus* egg extract supplemented with high nuclear concentrations (1500 sperm/μl) (Newport and Dasso, 1989). In our hands, 1200 sperm/μl was enough for a DNA replication checkpoint. CSF-released extracts were supplemented with 1200 sperm/μl and activated by 0.4 mM calcium (Fig. 10B). In the positive control (Fig. 10Ba), the CSF-released extract cycled through Meiosis II, interphase and Mitosis I. In the negative control (Fig 10B c), 100 μg/ml aphidicolin and 1200 sperm / μl sperm triggered a DNA replication checkpoint in CSF-released extract which arrested in interphase for the duration of the experiment (140 minutes). As shown in Fig. 10Bb, in the absence of aphidicolin, the activation threshold was 40 nM in cycloheximide-treated, CSF-released extract. However, in the presence of aphidicolin, 80 nM Δ87 cyclin B was not enough for activation (Fig. 10Bd). The activation threshold in aphidicolin-treated extract was 100 nM, 2.5 fold higher than in untreated extract. This data suggested that high concentration of human cyclin B1 protein is able to rescue the cell cycle from DNA replication checkpoint. However, the activation threshold is much higher than the activation threshold in extracts without a DNA replication checkpoint. This experiment thus confirmed the predicted effect of unreplicated DNA on the hysteresis loop.

4.3.2 DISCUSSION

In Novak-Tyson model, unreplicated DNA increases the threshold by increasing some phosphatases which activate Wee1 and inactivate Cdc25. However, according to recent reports, DNA replication checkpoint activates XChk1 which phosphorylates Cdc25 and Wee1 on Ser-287 and Ser-549, respectively. These phosphorylations result in the binding of 14-3-3 proteins to Cdc25 and Wee1. The binding of 14-3-3 proteins inhibits the nuclear import of Cdc25, thereby suppresses its ability to induce mitosis. The binding of 14-3-3 proteins to Wee1 stimulates the ability of Wee1 to phosphorylate Cdc2 and also promotes the distribution of Wee1 within the nucleus. (Kumagai et al., 1998; Kumagai and Dunphy, 1999; Lee et al., 2001)

Our experimental data verified Novak-Tyson's prediction regarding the increases in the activation threshold at DNA replication checkpoint. However, this prediction was based on some assumptions that we now know are inaccurate. In Novak-Tyson model, unreplicated DNA increases the activation threshold by increasing the activities of phosphatases called phosphatase b and phosphatase f, which dephosphorylate Cdc25 and Wee1, respectively (Novak and Tyson, 1993). This does not occur at a DNA replication checkpoint.

According to the current model for DNA replication checkpoint, Tyson recalculated the activation threshold at DNA replication checkpoint by increasing Wee1 concentration in nucleus and decreasing Cdc25 concentration in nucleus. The simulation result matched our experimental data: the activation threshold at DNA replication checkpoint is 2.5 fold higher than in untreated extract.

We asked: how could high cyclin B rescue the extract from the DNA replication checkpoint? This indicates that some Cdc25 activity is still present at the DNA replication checkpoint and it activates some pre-MPF (phosphorylated on Y15 and T14). This activated MPF may reverse the phosphorylation on Cdc25 Ser-287, which then could trigger the positive feedback and eventually activate the remaining pre-MPF and

drive the extracts into mitosis. The reversion of phosphorylation may also happen to Wee1 Ser-549. To confirm this hypothesis, some experiments may need to be performed in the future to measure the phosphorylation on Ser-287 and Ser-549 at the DNA replication checkpoint with or without high concentrations of cyclin B protein.

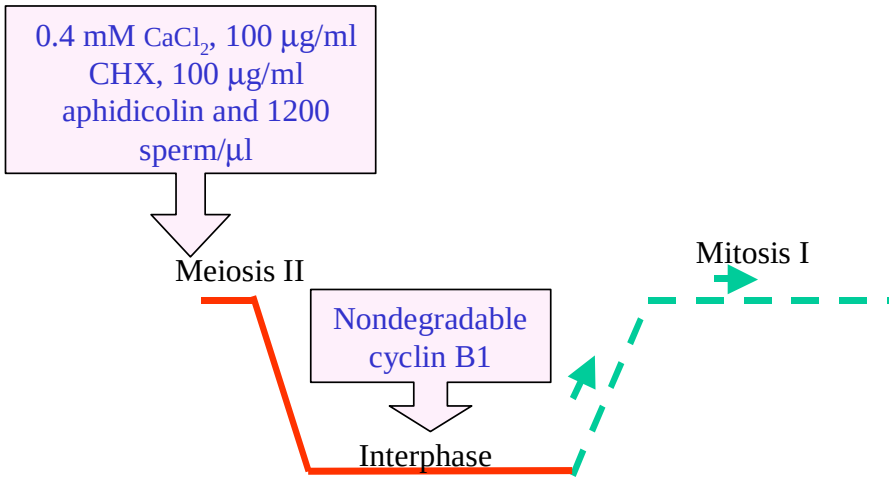

Fig. 10A. Experimental design for measuring the threshold at DNA replication checkpoint. 100 µg/ml cycloheximide, 100 µg/ml aphidicolin and 1200 sperm nuclei/ml were added to CSF released extract at 0 minutes. Different concentrations of Δ87 cyclin B protein were added to this extract when it entered interphase. The activation threshold was measured by sperm morphology.

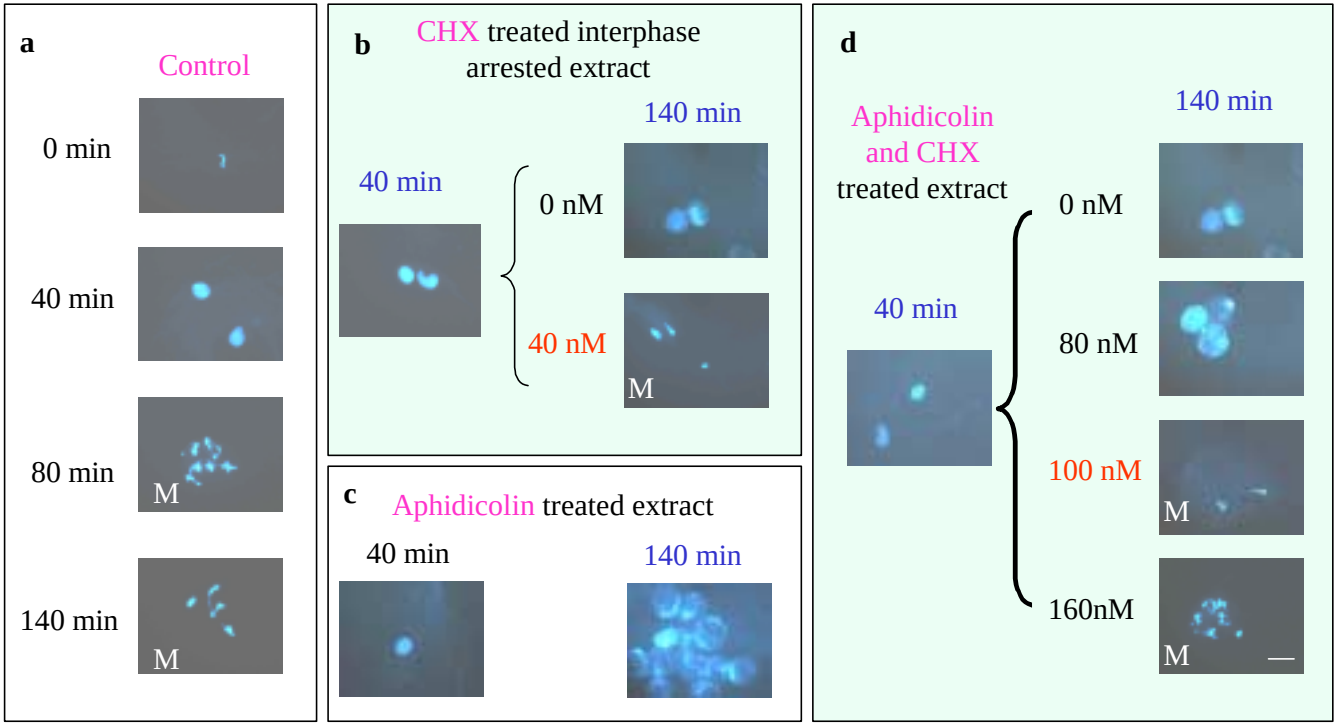

Fig. 10B. The activation threshold is increased when DNA replication checkpoint is engaged. a) control CSF-released extract. b) cycloheximide-treated, CSF-released extract. Δ87 cyclin B1 was added to this extract at 40 minutes (interphase). Samples were taken at 40 minutes and 140 minutes. c) Aphidicolin-treated, CSF-released extract. Samples were taken at 40 minutes and 140 minutes. d) Experiment was performed as described in Fig. 10A. Δ87 cyclin B1 was added to cycloheximide and aphidicolin treated CSF released extract at 40 minutes (interphase). Samples were taken at 40 minutes and 140 minutes. M = mitosis. Extracts are labelled M when >90% nuclei on slide appear mitotic (condensed chromatin and no nuclear envelope). Scale bar = 50 μm.

Chapter 5: CONCLUSION and PERSPECTIVES

These studies confirmed three fundamental predictions of the Novak-Tyson model of the mitotic cycle in cell-free extracts from *Xenopus* eggs. 1) The cyclin B level required for MPF activation is higher than the cyclin B level required for MPF inactivation. 2) The lag time for activation of MPF depends upon cyclin concentration at values close to the activation threshold. 3) The activation threshold is increased when DNA replication checkpoint is engaged. Therefore, hysteresis in MPF regulation is confirmed in *Xenopus* egg extract. This study confirms the value of mathematical analysis of complex biological control systems such as the eukaryotic cell cycle.

Despite its success, this model needs to be extended to include other proteins that we now know to play important roles in MPF activation and inactivation.

In 1996, Patra and Dunphy found that in *Xenopus* egg extracts, MPF is a trimeric complex consisting of Cdc2, cyclin B and a small 9-kDa subunit called Xe-p9, a homolog of the Suc1/Cks protein. Suc1/Cks protein is essential for the proper regulation of Cdc2 in various species (Patra and Dunphy, 1996; Moreno et al., 1989; Tang et al., 1993; Sudakin et al., 1997; Kaiser et al., 1999). In *Xenopus* egg extracts, p9 is required for both entry into and exit from mitosis (Patra and Dunphy, 1996).

The Pin1 protein has recently emerged as another potential regulator of mitotic progression (Lu et al., 1996; Ranganathan et al., 1997; Shen et al., 1998; Crenshaw et al., 1998; Lu et al., 1999). In *Xenopus* egg extract, excess Pin1 protein can antagonize the stimulatory effect of p9 on the phosphorylation of the regulators of Cdc2 and inhibit the entry into mitosis (Patra et al., 1999). Depletion of Pin 1 from human cells results in a defect in the progression through mitosis (Lu et al., 1996). These data collectively suggest that Pin 1, like p9, plays some role both in the entry into and progression through mitosis.

Plk 1 has been implicated in regulating both entry into M phase and exit from M phase. At the onset of mitosis, this kinase initiates the activation of the Cdc25C phosphatase that in turn dephosphorylates and activates Cdc2/cyclin B (Qian et al., 1998;

Abrieu et al., 1998; Karaiskou et al., 1999; Karaiskou et al., 1998). Moreover, Plk1 promotes the nuclear translocation of the Cdc2/cyclin B complex (Toyoshima-Morimoto et al., 2001). Upon exit from M phase, Plk activity appears to be important for the activation of the ubiquitin ligase known as anaphase promoting complex/cyclosome (APC) (Kotani et al., 1998; Kotani et al., 1999; Charles et al., 1998; Shirayama et al., 1998). In addition, Plk1 and its orthologs are implicated in centrosome maturation and spindle formation, as well as in signaling aspects of cytokinesis (reviewed in Nigg, 1998; Glover et al., 1998).

A recently discovered protein, Emi1, regulates mitosis by inhibiting the anaphase promoting complex/cyclosome (APC). Emi1 accumulates before mitosis and is ubiquitinated and destroyed in mitosis. Emi1 regulates progression through early mitosis by preventing premature APC activation, and may help explain the well-known delay between cyclin B/Cdc2 activation and cyclin B destruction (Reimann et al., 2001).

A second isoform of Cdc25, *Xenopus* Cdc25A, was cloned in 1999 (Kim et al., 1999). Unlike Cdc25C, which is present at constant level during early *Xenopus* development, the synthesis of Cdc25A begins within 30 minutes of fertilization, and the protein product accumulates continuously until the MBT, after which it is degraded. The dephosphorylation of Cdc2 and Cdk2 by Cdc25A plays an important role in controlling the length of the cell cycle.

The Novak-Tyson model has provided a valid framework for cell cycle control in *Xenopus* egg extract and a practical theoretical approach to the study of complex biological control system. However, the discovery of novel MPF regulators suggests that MPF regulation is more complex than what was described in 1993 by Novak and Tyson. Hence, there is a need to build more complex model of cell cycle control in the future.

REFERENCES

Abrieu, A., Fisher, D., Simon, M.N., Doree, M., and Picard, A. (1997). MAPK inactivation is required for the G2 to M-phase transition of the first mitotic cell cycle. EMBO J. 16, 6407-6413.

Abrieu, A., Brassac, T., Galas, S., Fisher, D., Labbe´ , J. C., and Dore´ e, M. (1998). The Polo-like kinase Plx1 is a component of the MPF amplification loop at the G2/M-phase transition of the cell cycle in *Xenopus* eggs. J. Cell Sci. 111, 1751–1757.

Arellano, M and Moreno, S. (1997) Regulation of CDK/cyclin complexes during the cell cycle. Int. J. Biochem. Cell Biol 29: 559-573.

Arion, D., Meijer, L., Brizuela, L. and Beach, D. 1988. *cdc2* is a component of the M phase-specific histone H1 kinase: Evidence for identity with MPF. *Cell* 55: 371—378.

Baitinger, C., Alderton, J., Poenie, M., Schulman, H., Steinhardt, R. A., (1990) Multifunctional Ca^{2+} / calmodulin–dependent protein kinase is necessary for nuclear envelope breakdown. J. Cell Biol. 111, 1763-1773.

Beckhelling, C., Penny, C., Clyde, S., Ford, C. (1999) Timing of calcium and protein synthesis requirements for the first mitotic cell cycle in fertilized Xenopus eggs. Journal of Cell Science 122, 3875-3984.

Beckhelling, C., Perez-Mongiovi, D and Houliston, E. (2000) Localised MPF regulation in eggs. Biology of the cell 92: 245-253.

Bhatt, R.R., and Ferrell, J.E. (1999). The protein kinase p90 rsk as an essential mediator of cytostatic factor activity. Science 286, 1362-1365.

Blow, J. J. and Nurse, P. (1990) A cdc2-like protein is involved in the initiation of DNA replication in Xenopus egg extracts. Cell 62, 855-862.

Borisuk, MT and Tyson, J. J. (1998) Bifurcation analysis of a model of mitotic control in frog eggs. J. theor. Biol. 195: 69-85

Charles, J. F., Jaspersen, S. L., Tinker-Kulberg, R. L., Hwang, L., Szidon, A., and Morgan, D. O. (1998). The Polo-related kinase Cdc5 activates and is destroyed by the mitotic cyclin destruction machinery in S. cerevisiae. Curr. Biol. 8, 497–507.

Ciapa B, Chiri S. (2000) Egg activation: upstream of the fertilization calcium signal. Biol Cell 92(3-4):215-33

Cisek, L. J. and Corden, J. L. 1989. Phosphorylation of RNA polymerase by the murine homologue of the cell-cycle control protein *cdc2. Nature* 339: 679—684

Coleman, T.R. and Dunphy, W.G. (1994) Cdc2 regulatory factors. Curr Opin Cell Biol. 6(6):877-82

Colledge, W.H., Carlton, M.B., Udy, G.B., and Evans, M.J. (1994). Disruption of c-mos causes parthenogenetic development of unfertilized mouse eggs. Nature 370, 65-68

Crenshaw, D. G., Yang, J., Means, A. R., and Kornbluth, S. (1998) The mitotic peptidyl-prolyl isomerase, Pin1, interacts with Cdc25 and Plx1. EMBO J. 17 (5), 1315–1327

Dasso, M., and Newport, J. W.,(1990) Completion of DNA replication is monitored by a feedback system that controls the initiation of mitosis *in vitro*: studies in *Xenopus*. Cell 61: 811-823

Dasso, M., Smythe, C., Milarski, K., Kornbluth, S. and Newport, J.W. (1992) DNA replication and progression through the cell cycle. The regulation of the Eudaryotic cell cycle, pp161-180. Chichester: John Wiley & sons.

Dettlaff, T. A. (1964) Cell divisions, duration of interkinetic states, and differentiation in early stages of embryonic development. Adv Morphogen 3, 323-362.

Draetta, G., Piwnica-Worms, H., Morrison, D., Druker, B., Roberts, T., Beach, D. Human cdc2 protein kinase is a major cell-cycle regulated tyrosine kinase substrate. Nature 336(6201):738-744

Dulic, V., Lees, E. and Reed, S. I. (1992) Association of human cyclin E with a periodic G sub(1)-S phase protein kinase. Science 257, 1958-1961.

Dunphy, W.G. and Newport, J.W. (1989) Fission yeast p13 blocks mitotic activation and tyrosine dephosphorylation of the Xenopus cdc2 protein kinase. Cell 58(1):181-191

Dunphy, W.G., and Kumagai, A. (1991). The cdc25 protein contains an intrinsic phosphatase activity. Cell 61, 189-196.

Evans, T., Rosenthal, E. T., Youngblom, J., Distel, D., and Hunt, T. (1983) Cyclin: a protein specified by maternal mRNA in sea urchin eggs that is destroyed at each cleavage division. Cell 33, 389-396.

Fang, F. and Newport, J. W. (1991) Evidence that the G1-S and G2-M transitions are controlled by different cdc2 proteins in higher eukaryotes. Cell 66, 731-742.

Featherstone, C., and Russell, P. (1991). Fission yeast $p107^{wee1}$ mitotic inhibitor is a tyrosine / serine kinase. Nature 349, 808-811.

Felix, M. A., Labbe, J. C., Doree, M., Hunt, T. and Karsenti, E. (1990) Triggering of cyclin degradation in interphase extracts of amphibian eggs by cdc2 kinase. Nature, 346, 379-382.

Furstenthal, L., Swanson, C., Kaiser, B. K., Aldridge, A. G. & Jackson, P. K. (2001) Triggering ubiquitination of a CDK inhibitor at origins of DNA replication. Nature Cell Biol. 3: 715-722.

Gautier, J., Minshull, J., Lohka, M., Glotzer, M., Hunt, T., and Maller, J.L. (1990). Cyclin is a component of maturation-promoting factor from *Xenopus*. Cell 60, 487-494.

Gautier, J., Solomon, M. J., Booher, R. N., Bazan, J. F. and Kirschner, M.W. (1991) Cdc25 is a specific tyrosine phosphatase that directly activates p34cdc2. Cell 67: 197-211.

Glotzer, M, Murray A. W. and Kirschner M. W. (1991) Cyclin is degraded by the ubiquitin pathway.?

Glover, D. M., Hagan, I. M., and Tavares, A. A. (1998). Polo-like kinases: A team that plays throughout mitosis. Genes Dev. 12, 3777–3787.

Gross, S.D., Schwab, M. S., Taieb, F.E., Lewellyn, A. L., Qian, Y. W., and Maller, J.L. (2000). The critical role of the MAP kinase pathway in meiosis II in *Xenopus* oocytes is mediated by p90 (Rsk). Curr. Biol., 10, 430-438.

Gurdon, J. B. (1976). Injected nuclei in frog oocytes: Fate, enlargement, and chromatin dispersal. J. Embryol. Exp. Morphol. 36, 523-540.

Haccard, O., Sarcevic, B., Lewellyn, A., Hartley, R., Roy, L., Izumi, T., Erikson, E., and Maller, J.L. (1993). Induction of metaphase arrest in cleaving *Xenopus* embryos by MAP kinase. Science 262, 1262-1265

Hartley, R. S., Sible, J. C., Lewellyn, A. L. and Maller, J. L. (1997) A role for cyclin E/Cdk2 in the timing of the midblastula transition in Xenopus embryos. Devel. Biol. 188

Izumi, T and Maller, J. L. (1993) Elimination of cdc2 phosphorylation sites in the cdc25 phosphatase blocks initiation of M-phase. Mol. Biol. Cell 4, 1337-1350.

Izumi, T., Walker, D.H. and Maller, J.L. (1992) Periodic changes in phosphorylation of the *Xenopus* cdc25 phosphatase regulate its activity. Mol. Biol. Cell 3, 927-939.

Kaiser, P., Moncollin, V., Clarke, D. J., Watson, M. H., Bertolaet, B. L., Reed, S. I., and Bailly, E. (1999) Cyclin-dependent kinase and Cks/Suc1 interact with the proteasome in yeast to control proteolysis of M-phase targets. Genes Dev. 13 (9), 1190–1202

Karaiskou, A., Jessus, C., Brassac, T., and Ozon, R. (1999). Phosphatase 2A and polo kinase, two antagonistic regulators of cdc25 activation and MPF auto-amplification. J. Cell Sci. 112, 3747–3756.

Karaiskou, A., Cayla, X., Haccard, O., Jessus, C., and Ozon, R. (1998). MPF amplification in *Xenopus* oocyte extracts depends on a two-step activation of cdc25 phosphatase. Exp. Cell Res. 244, 491–500.

Kay, Brian and Peng, Benjamin. (1991) *Xenopus* laevis: practical uses in cell and molecular biology ? Methods in Cell Biology, Volume 36. ?

Kim, S. H., Li, C., and Maller J. L. (1999) A maternal form of the phosphatase Cdc25A regulates early embryonic cell cyclies in *Xenopus* laevis. Dev Biol, 212(2): 381-389.

King RW, Peters JM, Tugendreich S, Rolfe M, Hieter P and Kirschner MW. (1995) A 20S complex containing CDC27 and CDC16 catalyzes the mitosis-specific conjugation of ubiquitin to cyclin B. Cell 81 (2):279-88

King, R. W., Deshaies, R.J., Peters, JM and Kirschner, M.W. (1996) How Proteolysis Drives the cell cycle. Science 274(5293): 1652-1659

Koff, A., Giordano, A., Desai, D., Yamashita, K., Harper, J. W., Elledge, S., Nishimoto, T., Morgan, D. O., Franza, B.R. and Roberts, J. M. (1992) Formation and activation of a cyclin E-Cdk2 complex during the G1 phase of the human cell cycle. Science 257, 1689-1694.

Kotani, S., Tugendreich, S., Fujii, M., Jorgensen, P. M., Watanabe, N., Hoog, C., Hieter, P., and Todokoro, K. (1998). PKA and MPF-activated polo-like kinase regulate anaphase-promoting complex activity and mitosis progression. Mol. Cell 1, 371–380.

Kotani, S., Tanaka, H., Yasuda, H., and Todokoro, K. (1999). Regulation of APC activity by phosphorylation and regulatory factors. J. Cell Biol. 146, 791–800.

Kumagai, A and Dunphy, W. G. (1991) The cdc25 protein controls tyrosine dephosphorylation of the cdc2 protein in a cell-free system. Cell 64: 903-914.

Kumagai, A. and Dunphy, W. G. (1992) Regulation of the cdc25 protein during the cell cycle in *Xenopus* extracts. Cell 70, 139-151

Kumagai, A. and Dunphy, W. G. (1995) Control of the Cdc2/cyclin B complex in *Xenopus* egg extracts arrested at a G2/M checkpoint with DNA synthesis inhibitors. Mol. Biol. Cell 6, 199-213.

Kumagai, A., and Dunphy, W.G. (1999). Binding of 14-3-3 proteins and nuclear export control the intracellular localization of the mitotic inducer Cdc25. Genes Dev. 13, 1067-1072.

Kumagai, A., Guo, Z., Emami, K. H., Wang, S. X., and Dunphy, W.G. (1998) The *Xenopus* Chk1 protein kinase mediates a caffeine-sensitive pathway of checkpoint control in cell-free extracts. J. Cell Biol. 142, 1559-1569

Langan, T.A., Gautier, J., Lohka, M., Hollingsworth, R., Moreno, S., Nurse, P., Maller, J., and Sclafani, R.A. (1989). Mammalian growth-associated H1 histone kinase: A homolog of cdc2/cdc28 protein kinase controlling mitotic entry in yeast and frog cells. Mol. Cell. Biol. 9, 3860-3868

Lee, J., Kumagai, A. and Dunphy, W. G. 2001 Positive regulation of Wee1 by Chk1 and 14-3-3. Molecular Biology of the Cell. Vol.12, 551-563

Leresche, A., Wolf, V. J., Gottesfeld, J.M. (1996) Repression of RNA polymerase II and III transcription during M phase of the cell cycle. Exp. Cell Res.: 229(2):282-8

Lindsay, H. D., Whitaker, M. J., Ford, C. C. (1995) Calcium requirements during mitotic cdc2 kinase activation and cyclin degradation in *Xenopus* egg extracts. J. Cell. Sci. 108, 3557-3568.

Lorca, T., Cruzalegui, F.H., Fesquet, D., Cavadore, J.C., Mery, J., Means, A., and Doree, M. (1993). Calmodulin-dependent protein kinase II mediates inactivation of MPF and CSF upon fertilization of *Xenopus* eggs. Nature 366, 270-273

Lohka, M. J., Hayes, M. K., & Maller, J. L. (1988). Purification of maturation-promoting factor, an intracellular regulator of early mitotic events. Proc. Natl. Acad. Sci. USA 85: 3009-3013.

Lohka, M. J., and Masui, Y. (1983). Formation in vitro of sperm pronuclei and mitotic chromosomes induced by amphibian ooplasmic components. Science 220: 719-721.

Lorca, T., Castro, A., Martinez, A. M., Vigneron, S., Morin, N., Sigrist, S., Lehner, C., Doree, M. and Labbe, J.C. (1998) Fizzy is required for activation of the APC/cyclosome in Xenopus egg extracts. The EMBO Journal. 17(13): 3565-3575.

Lorca, T., Cruzalegui, F.H., Fesquet, D., Cavadore, J-C., Mery, J., Means, A. and Doree, M. (1993) Calmodulin-dependent protein kinase II mediates inactivation of MPF and CSF upon fertilization of Xenopus eggs. Nature 366, 270-273.

Lu, K. P., Hanes, S. D., and Hunter, T. (1996) A human peptidyl-prolyl isomerase essential for regulation of mitosis. Nature 380 (6574), 544–547

Lu, P. J., Zhou, X. Z., Shen, M., and Lu, K. P. (1999) Function of WW domains as phosphoserine- or phosphothreonine-binding modules. Science 283 (5406), 1325–1328

Marlovits, G. (1998) Modeling M-phase control in *Xenopus* oocyte extracts: the surveillance mechanism for unreplicated DNA. Biophys. Chem. 72, 169-184.

Masui, Yoshio and Wang, Ping. (1998) Cell cycle transition in early embryonic development of *Xenopus* Laevis. Biology of the Cell. 90 (8): 537-548.

McGowan, C.H., and Russell, P. (1995). Cell cycle regulation of human WEE1. EMBO J. 14, 2166-2175.

Miake-Lye, R. and Kirschner, M. W. 1985. Induction of early mitotic events in a cell-free system. *Cell* 41: 165—175.

Minshull, J., Blow, J. J., and Hunt, T. (1989) Translation of cyclin mRNA is necessary for extracts of activated *Xenopus* eggs to enter mitosis. Cell 56, 947-956.

Moreno, S., Hayles, J., and Nurse, P. (1989) Regulation of p34cdc2 protein kinase during mitosis. Cell 58 (2), 361–372

Mueller, P.R., Coleman, T.R. and Dunphy,W.G. (1995a) Cell cycle regulation of a *Xenopus* Wee1-like kinase. Mol. Biol. Cell 6:119-134.

Mueller, P.R., Coleman, T.R. Kumagai, A. and Dunphy, W.G. (1995b) Myt1: a membrane-associated inhibitory kinase that phosphorylates Cdc2 on both threonine-14 and tyrosine-15. Science 270: 86-90.

Murray, A. W. & Kirschner, M.W. (1989) Cyclin synthesis drives the early embryonic cell cycle. NATURE. VOL 339. 275-280.

Murray, A. W., Solomon, M. J., and Kirschner, M. W. the role of cyclin synthesis and degradation in the control of maturation promoting factor activity. Nature. Vol 339. 280-285.

Murray, A.W. (1991) Methods in cell biology, Volume 36: Xenopus laevis: practical uses in cell and molecular biology. Edited by Kay, B.K. and Peng, H.B. Chapter 30: Cell Cycle Extracts.

Murray, A and Hunt, T. (1993) The Cell Cycle, an introduction. New York: W. H. Freeman Co.

Nebreda, A.R., and Hunt, T. (1993). The c-mos proto-oncogene protein kinase turns on and maintains the activity of MAP kinase, but not MPF, in cell-free extracts of *Xenopus* oocytes and eggs. EMBO J. 12, 1979-1986

Newport, J. and Dasso, M. (1989) On the coupling between DNA replication and mitosis. J. Cell Sci. Suppl. 12, 149-160.

Nigg, E. A. (1998). Polo-like kinases: Positive regulators of cell division from start to finish. Curr. Opin. Cell Biol. 10, 776–783.

Novak, B and Tyson, J. J. (1993) Numerical analysis of a comprehensive model of M-phase control in *Xenopus* oocyte extracts and intact embryos. J. Cell Sci. 106:1153-1168.

Novak. B. and Tyson, J. J. (1995) Quantitative analysis of a molecular model of M-phase control in *Xenopus* oocyte extracts and intact embryos. J. Theor. Biol. 173, 283-305.

Novak, B and Tyson, J. J. (1997) Modeling the control of DNA replication in fission yeast. Proc. Natl. Acad. Sci. USA 94:9147-9152.

Novak, B and Tyson, J. J. (1998) Mathematical model of the fission yeast cell cycle with chechpoint controls at the G1/S, G2/M and metaphase/anaphase transitions. Biophys. Chem. 72: 185-200.

Pagano, M., Pepperkok, R., Verde, F., Ansorge, W., and Draetta, G. (1992). Cyclin-A is required at two points in the human cell cycle. EMBO J. 11, 961-971.

Parker, L.L., and Piwnica-Worms, H. (1992). Inactivation of the $p34^{cdc2}$-cyclin B complex by the human WEE1 tyrosine kinase. Science 257, 1955-1957.

Patel, R., Holt, M., Philipova, R., Moss, S., Schulman, H., Hidaka, H., Whitaker, M. (1999) Calcium/calmodulin-dependent phosphorylation and activation of human Cdc25 – C at the G2/M phase transition in Hela cells. J. Biol. Chem 274, 7958-7968.

Patra, D., and Dunphy, W. G. (1996) Xe-p9, a Xenopus Suc1/Cks homolog, has multiple essential roles in cell cycle control. Genes Dev. 10 (12), 1503–1515

Patra, D. and Dunphy, W. G. (1998) Xe-p9, a Xenopus Suc1/Cks protein, is essential for the Cdc2-dependent phosphorylation of the anaphase-promoting complex at mitosis. Genes Dev. 12, 2549-2559.

Patra, D., Wang, S. X., Kumagai, A. and Dunphy. W.G. (1999) The *Xenopus* Suc1/Cks protein promotes the phosphorylation of G2/M regulators. The Journal of biological chemistry, 274 (52) 36839-36842.

Peter, M., Nakagawa, J., Dorée, M., Labbé, J. C. and Nigg, E. A. 1990. *In vitro* disassembly of the nuclear lamina and M phase-specific phosphorylation of lamins by cdc2 kinase. *Cell* 61: 591—602.

Pines, J., and Hunt, T. (1987) Molecular cloning and characterization of the mRNA for cyclin from sea urchin eggs. EMBO J. 6, 2987-2995.

Posada, J., Yew, N., Ahn, N.G., Vande Woude, G.F., and Cooper, J.A. (1993). Mos stimulates MAP kinase in *Xenopus* oocytes and activates a MAP kinase kinase in vitro. Mol. Cell. Biol. 13, 2546-2553

Qian, Y. W., Erikson, E., Li, C., and Maller, J. L. (1998). Acti-vated polo-like kinase Plx1 is required at multiple points during mitosis in *Xenopus* laevis. Mol. Cell Biol. 18, 4262–4271.

Ranganathan, R., Lu, K. P., Hunter, T., and Noel, J. P. (1997) Structural and functional analysis of the mitotic rotamase Pin1 suggests substrate recognition is phosphorylation dependent. Cell 89, 875–886

Reimann, J.D., Freed, E., Hsu, J.Y., Kramer, E.R., Peters, J.M., Jackson, P.K. (2001) Emi1 is a mitotic regulator that interacts with Cdc20 and inhibits the anaphase promoting complex. Cell 105(5):645-655

Roy, L.M., Haccard, O., Izumi, T., Lattes, B.G., Lewellyn, A.L., and Maller, J.L. (1996). Mos proto-oncogene function during oocyte maturation in *Xenopus*. Oncogene *12*, 2203-2211

Santella, L., (1998) The role of calcium in the cell cycle: facts and hypotheses. Biochem. Biophys. Res. Commun. 244, 317-324.

Satoh, N (1977) 'Metachronous' cleavage and initiation of gastrulation in amphibian embryos. Dev Growth Differ 19, 111-118

Satterwhite, L. L., Lohka, M. J., Wilson, K. L., Scherson, T. Y., Cisek, L. J. and Pollard, T. D. 1992. Phosphorylation of myosin-II light chain by cyclin-p34^{cdc2}: A mechanism for the timing of cytokinesis. *J. Cell Biol.* 118: 595—605.

Shen, M., Stukenberg, P. T., Kirschner, M. W., and Lu, K. P. (1998) The essential mitotic peptidyl-prolyl isomerase Pin1 binds and regulates mitosis-specific phosphoproteins. Genes Dev.12, 706–720.

Shibuya, E.K., and Ruderman, J.V. (1993). Mos induces the *in vitro* activation of mitogen-activated protein kinases in lysates of frog oocytes and mammalian somatic cells. Mol. Biol. Cell 4, 781-790

Shirayama, M., Zachariae, W., Ciosk, R., and Nasmyth, K. (1998). The Polo-like kinase Cdc5p and the WD-repeat protein Cdc20p/fizzy are regulators and substrates of the anaphase promoting complex in Saccharomyces cerevisiae. EMBO J. 17, 1336–1349.

Shou,W. and Dunphy,W.G. (1996) Cell cycle control by Xenopus p28Kix1, a developmentally regulated inhibitor of cyclin-dependent kinases. Mol. Biol. Cell 7 (3), 457-469.

Smythe, C. and Newport, J.W. (1992). Coupling of mitosis to the completion of S phase in *Xenopus* occurs via modulation of the tyrosine kinase that phsphorylates P34cdc2. Cell 68, 787-797.

Solomon, M. J., Glotzer, M., Lee, T. H., Phillippe, M and Kirschner, M. W. (1990) Cyclin activation of p34 cdc2. Cell 63: 1013-1024

Solomon, M. J. (1994) The function(s) of CAK, the p34cdc2-activating kinase. Trends Biochem Sci. 1994 Nov;19(11):496-500.

Su, J. Y., Rempel, R. E., Erikson, E. and Maller, J. L. (1995) Cloning and characterization of the Xenopus cyclin-dependent kinase inhibitor p27XIC1. Proc. Natl. Acad. Sci. U.S.A. 92 (22), 10187-10191

Sudakin V, Ganoth D, Dahan A, Heller H, Hershko J, Luca FC, Ruderman JV and Hershko A. (1995) The cyclosome, a large complex containing cyclin-selective ubiquitin ligase activity, targets cyclins for destruction at the end of mitosis. Mol Biol Cell 1995 Feb;6(2):185-97

Sudakin, V., Shteinberg, M., Ganoth, D., Hershko, J., and Hershko, A. (1997). Binding of activated cyclosome to p13(suc1). Use for affinity purification. J. Biol. Chem. 272 (29), 18051–18059

Tang, Y., and Reed, S. I. (1993) The Cdk-associated protein Cks1 functions both in G1 and G2 in Saccharomyces cerevisiae. Genes Dev. 7 (5), 822–832

Toyoshima-Morimoto, F., Taniguchi, E., Shinya, N., Iwamatsu, A., and Nishida, E. (2001). Polo-like kinase 1 phosphorylates cyclin B1 and targets it to the nucleus during prophase. Nature 410, 215–220.

Tyson, J. J. (1991) Modeling the cell division cycle: cdc2 and cyclin interactions. Proc. Natl. Acad. Sci. USA 88, 7328-7332.

Walker, D. H. and Maller, J. L. (1991). Role for cyclin A in the dependence of mitosis on completion of DNA replication. Nature 354, 314-317.

Ward, G. E. and Kirschner, M. W. 1990. Identification of cell cycle-regulated phosphorylation cites on nuclear lamin C. Cell 61: 561—577.

Watanabe, N., Hunt, T., Ikawa, Y., and Sagata, N. (1991). Independent inactivation of MPF and cytostatic factor (Mos) upon fertilization of *Xenopus* eggs. Nature 352, 247-248

Watanabe, N., Broome, M., and Hunter, T. (1995). Regulation of the human WEE1Hu CDK tyrosine 15-kinase during the cell cycle. EMBO J. 14, 1878-1891.

Yamashiro, S., Matsumura, F., (1991) Mitosis-specific phosphorylation of caldesmon: possible molecular mechanism of cell rounding during mitosis. Bioessays 13(11):563-568

You, Z., Harvey, K., Kong, L., Newport, J. (2002) Xic1 degradation in Xenopus egg extracts is coupled to initiation of DNA replication. 16(10) 1182-1194

VITA

Wei Sha

Education

- Capital University of Medical Sciences, Beijing, P.R. China; Bachelor of Medicine, Major: Pediatrics; July 1993 - July 1998
- Virginia Tech, Master of Science in Biology; January 2000 – August 2002

Research Experience

January 2000 – August 2002

Testing mathematical model that relates cyclin B level to MPF activity in *Xenopus* egg extracts.

Master's Thesis: "Experimental evidence for hysteresis in the cell cycles of *Xenopus Laevis* egg extracts"

Principal Investigator: Jill C. Sible

Teaching Experience

January 2001 – May 2001

Teaching General Biology Lab (BIOL 1116)

Abstracts

- The Cell Cycle

  Cold Spring Harbor, NY, May 15-19, 2002

  "Experimental evidence for hysteresis in the cell cycle of *Xenopus Laevis* egg extracts"

- American Cancer Society meeting of cancer researchers in Virginia

  Blacksburg, VA, April 13, 2002

  "Testing hysteresis in the cell cycle of *Xenopus Laevis* egg extracts"

- Molecular Biology of the Cell Cycle course

  Virginia Tech, October 11, 2001

  “The phosphorylation of p53 by Chk1 and Chk2”

- Cell Biology Journal Club

  Virginia Tech, October, 3, 2001

  “Cytolethal Distending Toxin, a Newly Discovered Inhibitor of the Cell Cycle”

- American Society of Cell Biology; Poster

  San Francisco, CA; Dec. 2000

  “Testing Mathematical Model that Relates Cyclin B mRNA Level to MPF Activity in Frog Egg Extracts”

Membership

American Society of Cell Biology membership